AD-A062 755 GENERAL SENSORS INC FORT WASHINGTON PA F/G 8/1
STUDY OF THE FEASIBILITY OF USING AN ADVANCED OPTO-ELECTRONIC I--ETC(U)
NOV 78 H SADJIAN N00014-77-C-0344
UNCLASSIFIED 6S-1-78-ONR NL

1 OF 2
AD A062755

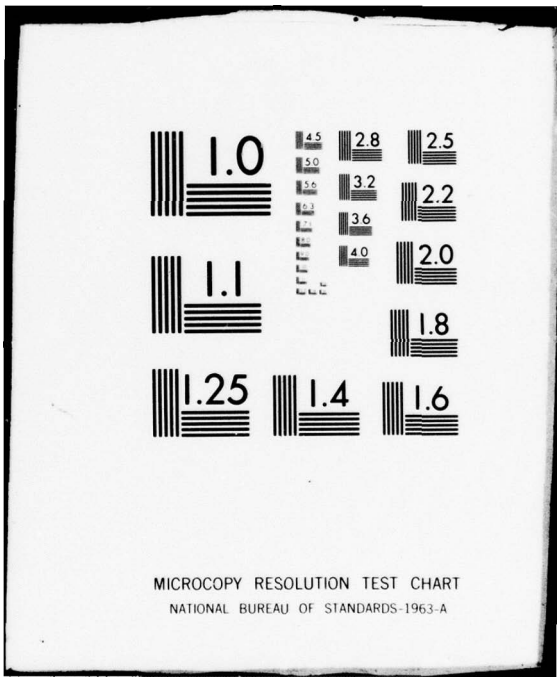
1.0
1.1
1.25
1.4
1.6
1.8
2.0
2.2
2.5
2.8
3.2
3.6
4.0
4.5
5.0
5.6
MICROCOPY RESOLUTION TEST CHART
NATIONAL BUREAU OF STANDARDS-1963-A

Report GS-ONR-1-78

(12)

GENERAL SENSORS, INC.

STUDY OF THE FEASIBILITY OF USING AN ADVANCED OPTO-ELECTRONIC IMAGING TECHNIQUE FOR SAMPLING MID-WATER NEKTON

LEVEL II

Harry Sadjian
GENERAL SENSORS, INC.
500 Office Center Drive
Ft. Washington, Pa. 19034

30 November 1978

Annual Report for Period 2 May 1977 - 30 September 1978

Approved for public release; distribution unlimited

Prepared for
OFFICE OF NAVAL RESEARCH
Dept. of the Navy
Arlington, Virginia 22217

Report GS-ONR-1-78

STUDY OF THE FEASIBILITY OF USING AN ADVANCED OPTO-ELECTRONIC IMAGING TECHNIQUE FOR SAMPLING MID-WATER NEKTON

Harry Sadjian
GENERAL SENSORS, INC.
500 Office Center Drive
Ft. Washington, Pa. 19034

30 November 1978

Annual Report for Period 2 May 1977 - 30 September 1978

Approved for public release; distribution unlimited

Prepared for
OFFICE OF NAVAL RESEARCH
Dept. of the Navy
Arlington, Virginia 22217

UNCLASSIFIED
SECURITY CLASSIFICATION OF THIS PAGE *(When Data Entered)*

REPORT DOCUMENTATION PAGE

READ INSTRUCTIONS BEFORE COMPLETING FORM

1. REPORT NUMBER: GS-ONR-1-78
2. GOVT ACCESSION NO.:
3. RECIPIENT'S CATALOG NUMBER: 9

4. TITLE *(and Subtitle)*: STUDY OF THE FEASIBILITY OF USING AN ADVANCED OPTO-ELECTRONIC IMAGING TECHNIQUE FOR SAMPLING MID-WATER NEKTON. (6)

5. TYPE OF REPORT & PERIOD COVERED: Annual rept. 2 May 1977- 30 Sept 1978

6. PERFORMING ORG. REPORT NUMBER:

7. AUTHOR(s): Harry Sadjian (10)

8. CONTRACT OR GRANT NUMBER(s): N00014-77-C-0344 new, N00014-78-C-0253 (15)

9. PERFORMING ORGANIZATION NAME AND ADDRESS:
General Sensors, Inc.
500 Office Center Drive
Ft. Washington, Pa. 19034

10. PROGRAM ELEMENT, PROJECT, TASK AREA & WORK UNIT NUMBERS: (11)

11. CONTROLLING OFFICE NAME AND ADDRESS:
Office of Naval Research Code: N00014
Dept. of the Navy 613C:DKB
Arlington, Virginia 22217

12. REPORT DATE: 30 November 1978

13. NUMBER OF PAGES: ix + 102 (12) 114p.

14. MONITORING AGENCY NAME & ADDRESS *(if different from Controlling Office)*: (14) GS-1-78-ONR

15. SECURITY CLASS. *(of this report)*: UNCLASSIFIED

15a. DECLASSIFICATION/DOWNGRADING SCHEDULE: N/A

16. DISTRIBUTION STATEMENT *(of this Report)*

Approved for public release; distribution unlimited

17. DISTRIBUTION STATEMENT *(of the abstract entered in Block 20, if different from Report)*

18. SUPPLEMENTARY NOTES

19. KEY WORDS *(Continue on reverse side if necessary and identify by block number)*
Nekton sampling
Pattern recognition
Myctophid characteristics
Sea water optical characteristics
Sea water optical imaging
Sea water imaging simulation

20. ABSTRACT *(Continue on reverse side if necessary and identify by block number)*

The feasibility of identifying mid-water nekton at 100 meters in clear ocean water using a fan shaped laser beam in conjunction with a photodiode array detector in a towed system is examined. It has been found that for myctophids and euphasiids, identification can be made only at ranges of 10 to 20 meters and is detector and light source limited. Calculations are presented that show the need for either computer or optical pattern recognition for the rapid identification and counting of these nekton. Both geo-

DD FORM 1 JAN 73 1473 EDITION OF 1 NOV 65 IS OBSOLETE

UNCLASSIFIED
SECURITY CLASSIFICATION OF THIS PAGE *(When Data Entered)*

410 437 78 100

4B

20. ABSTRACT (cont'd)

metric and bioluminescent characteristics are examined as possible candidates for recognition parameters. At high tow rates(about 10 knots), the need for optical pattern recognition has been found to be necessary. Methods are suggested for both optical pattern recognition and sea water optical characteristic simulation to evaluate developed optical recognition systems for myctophids.

An appendix presents general characteristics of mid-water nekton with an analysis of the electronic transmission requirements and limitations at mid-water depths. A selected bibliography is also presented on mid-water nekton.

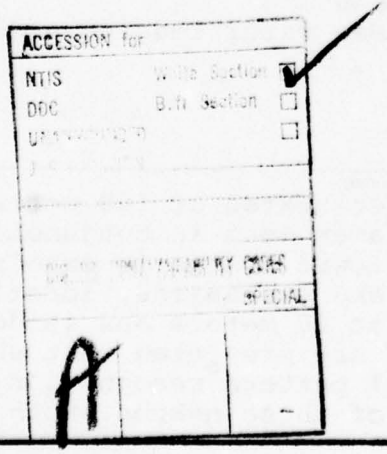

GS-ONR-1-78 30 November 1978

STUDY OF THE FEASIBILITY OF USING AN ADVANCED OPTO-ELECTRONIC IMAGING TECHNIQUE FOR SAMPLING MID-WATER NEKTON

The motivation and need for developing a system for recognizing and counting mid-water nekton using pattern recognition stems from need of developing new sampling techniques as a result of the, "Workshop On Problems Of Assessing Population Of Nekton", held in Santa Barbara, Calif. in 1975 sponsered by ONR and the National Science Foundation.

The initial phase of this work (approximately 4 months) conducted under Contract No. N00014-77-C-0344, was concerned with the study of the image requirements for developing "intelligence" for identifying small mid-water nekton in a towed system currently being developed by the Navy. This phase addressed the problem of resultant image quality and requirements for identification. This preliminary study has indicated that a towed system must operate within 10 to 20 meters of the nekton with the myctophids and the euphasiids representing the lower limit of nekton recognition. For rapid identification, a pattern recognition hierarchy is found to be necessary. Both geometric and bioluminecent characteristics of the myctophids were examined as possible candidate recognition parameters.

The second phase of this work (approximately 3 months) conducted under Contract No. N00014-78-C-0253 addressed the problem of high tow rates. It has been found that at tow rates of up to 10 knots that optical pattern recognition is necessary as computer pattern recognition cannot meet the high data transfer rate requirements. Suggestions are made on the technique to be used for accomplishing optical pattern

recognition of myctophids. In addition, it is shown how the sea water optical characteristics can be simulated optically to assess the ability of optical pattern recognition techniques to identify myctophids or other small nekton.

An appendix presents general nekton characteristics with an analysis of the electronic requirements for data transmission through a cable at mid-water depths. A selected bibliography on mid-water nekton is also presented.

Grateful acknowledgement is herewith given to Dr. Eric Softley of Ocean Applications Systems, Inc. at Key Biscayne, Florida for the data transmission analysis and to Mr. Roland Starkey of Environs Systems, Inc. at Exton, Pa. for conducting the literature survey on mid-water nekton characteristics. In addition, we are pleased to acknowledge the encouragement and guidance provided by Lt. T. Christtensen of ONR at Bay St. Louis, Miss. who was the project monitor of the first phase of this study. We also wish to express our gratitude to Dr. E. Silva of ONR in Arlington, Va. for his support and encouragement given to us during the course of the second phase of this study and for allowing us the opportunity to pursue this very challenging and unique approach to the sampling problem.

We also wish to give a special thanks for the contribution made by Mr. Ronald K. Amiraian, a college student who worked with us during the summer of 1977. His dedication in preparing most of the figures and curves of this report is greatly appreciated even though we are deeply saddened to make this acknowledgement posthumously. We humbly dedicate this effort to his memory.

TABLE OF CONTENTS

TABLE OF CONTENTS (cont'd)

I INTRODUCTION

The study of the marine ecology requires quantitative estimates on the standing stocks of nekton to assist in evaluating the structure and dynamics of marine ecosystems. Nekton populations comprise a large portion of the living biomass and may have a major role in recycling of elements and regulating the structure of population at lower trophic levels.

As no one method of sampling is adequate for an understanding of the nekton role in the marine ecosystem, a judicious mix of techniques and technologies that complement each other could increase the ability to assess nekton populations.

For the basis of the ensuing discussion,meso-pelagic(mid-water) nekton includes animals capable of moving from place to place between 200 to 2000 meters. By definition, this consists primarily of vertebrates(fish),squid(Cephalopods) and some forms of higher crustaceans(Decapods). The great mass of invertebrates is excluded due to the lack of directed and sustained locomotion.

Quantitative analysis of nekton populations can provide valuable data pertinent to food web composition, estimation of commercial and sports fisheries harvest and investigation of bioacoustics phenomena.

Sampling per se in meso-pelagic waters is compounded by the lack of a single technique capable of providing reliable identification and enumeration of all species within a search area. Basically, the problem can be defined in terms of biological and non-biological factors limiting the suitability of equipment currently being used for this purpose:[1]

TRAWLS

Mid-water trawls of the U.S. fleet are limited to small pelagic animals due to inadequate nets (~200 meters^2 mouth opening) and the inability to sample at discrete depths. Net avoidance is observed among strong swimmers and can only be overcome in part by using 1600 mesh nets with mouth openings of 1000 meters^2 or larger. Operation of such nets is very expensive as well as requiring specially equipped vessels for their deployment.

EGG AND LARVAL STUDIES

Low cost ichthyoplankton surveys have been popularized for investigating population dynamics of fishes, detection and appraisal of fishery resources and studies in biology and systematics. Abundance and distribution of adults can only be monitored by this method in the spawning area during the spawning season. Sampling is generally considered to be very poor in surveys of this type compared to that obtained by acoustic eggs or larvae, or being demersal in nature, would not be detected by this method. Thus, the value of mid-water ichthyoplankton surveys in estimating adult biomass is seriously limited.

ACOUSTICAL TECHNIQUES

Low frequency (broadband systems) studies of mesopelagic nekton provide excellent information on the presence or absence of fish with swim bladders. In particular this has provided detailed insight into the vertical migration(diurnal) of Mycophidae and siphonophores of the suborder Physonectae.

The former, characterized by lantern fish, have a gas-filled swim bladder resonant for sound pulses from 12 to 24 kHz. Physonectae, polymorphic coelenterates containing bubbles of carbon monoxide, similarly respond to echo sounder frequencies. Although acoustical techniques for assessment of nektonic populations provide acceptable levels and continuity of sampling, the method had has several short comings: Fish without swim bladders can not be detected and species identification and packing densities requires anciliary data as trawls for verification.

REMOTE SENSING

Direct aerial observations and photography, including multispectral imaging, are limited to nekton in epipelagic waters under the best of environmental conditions. Some fish are known to have unique spectral signatures and can be identified from the air. Tuna schools are routinely tracked at night and biomass estimates made by virtue of the intensity of the bioluminescent signal from disturbed waters. This would not be seen under conditions of ambient lighting or adverse weather conditions. Again, anciliary information is required to confirm the accuracy of the airborne data.

DIRECT OBSERVATION BY SUBMERSIBLES, TELEVISION AND PHOTOGRAPHIC METHODS

Valuable data has been obtained from submersibles in the mesopelagic zone and has provided basic information on the vertical (diurnal) migration of sound scattering layers. Unfortunately use of such craft is not practical for large area surveys due

to the limited "window" (sampling area) for TV,cameras and observers. The latter may not be able to identify all nekton observed and sample collection capability is usually quite limited. It also appears that some nekton may avoid submersibles,possibly due to lights,motor sounds etc. and only be seen as a matter of chance. Based on comparison of operational costs and the amount of data retrieval, submersibles are highly impractical for meso-pelagic surveys. Populations have been surveyed by operation of conventional remote surveillance systems; however, concern exists that studies of motile animals may similarly be influenced by sounds,lights and mechanical disturbances.

FOOD HABITS

Examination of the stomach of carnivores, e. g., seals, sperm whales, dolphins and porpoises, salmon etc., can provide valuable information regarding nektonic composition throughout the water column. In many instances large and small nekton infrequently caught in nets are extensively seen in the stomachs of sperm whales and Alepisaurus sp., respectively. Based on the aforegoing it can be readily seen that non of the techniques currently in use can satisfactorily provide unbiased and statistically valid profiles of meso-pelagic nekton. Common problems shared in most cases include:

1. Inadequacy of sample.
2. Aversion phenomena associated with environmental disturbances (light, sound and /or mechanical).
3. Difficulty of correlating survey methods with species identity and density of biomass.

4. Lack of real-time capability for vertical and horizontal profiling.
5. Requirement for manual sorting of trawls and species identification by taxonomista.
6. High cost in relationship to the quality and quantity of data.

It is not expected that a new system can circumvent all of the problems, but suggest that the "window" of an advance nekton optical monitoring system would be comparable to an 1000 m^2 opening of nets currently in use on West German, Polish and Soviet research vessels.

Although net sampling is the most direct sampling technique, it appears that the avoidance of motile animals and bias produced by the net size is a serious problem. In order to augment the net sampling technique and to obvia e the disadvantages of the systems indicated above, the development of an opto-electronic imaging system using an optical pattern recognition scheme to be used in conjunction with an existing towed fish is desirable that:

a. produces a mouth opening equivalent to that encompassed by large nets
b. uses monochromatic light which minimizes the effect of lights on motile animals characteristic of white light sources
c. provides the requisite recognition parameties to identify and count nekton density
d. minimizes backscattering which limits contrast in conventional TV systems

e. transmits only useful information therby reducing information storage capacity

A possible scenario is depicted in Figure 1. Here a research vessel (mother ship) suitably modified to provide a platform to station the controls for a towed fish (sensor) is indicated. The controls may consist of a suitable display, microcomputer, receiver and transmitter. The cable is used to deploy the towed fish and to transmit power and receive data from the fish. The towed fish may also consist of a laser source (operated in pulsed or CW mode), a viewing system, an electronic film plane (e.g. photodiode array) and an electronic processing unit.

The laser source (e.g. argon, He/Cd or doubled YAG) is chosen for its ability to be pulsed or run continuously. The laser light emanates from one end of the towed fish and the viewing system is located at the other end providing a seperation of source and viewing system of about 10 meters. The laser beam is shaped into a fan of light by suitable optics (i.e. sheet of light) which diverges in one direction and is essentially collimated in the other direction. In addition, it is moved mechanically (e.g. rotating mirror) to provide a scan angle for the fan beam sweeping out an unsymmetrical wedge shaped volume. The viewing system is also scanned mechanically in synchronism with the scanning light source.

The scanning light source and viewing system share a common volume. This methode of operation reduces back scattering to such an extent that the viewing range is about 6 attenuation lengths. For clear ocean water (attenuation coefficient alpha about .05 meter^{-1}), this corresponds to a range of about 120 meters. If a pencil of light is used, the range can be extended to about 7 attenuation lengths; however, the increased complexity of the resulting system does not

warrant it. For simple TV type flood light illumination, depending on the water turbidity, it is about 4.5 attenuation lengths. It is believed that a dual synchronism scan system for imaging represents the best compromise between sensor complexity and range.

Although there are many variables that will affect the performance of the viewing system described above (e.g. water turbidity, contrast of the fish, efficiency of the overall viewing system and resolution and range requirements), it is believed that such a system augmented by a suitable pattern recognition system would represent a quantum jump in the way sampling is conducted for mid-water nekton.

In the following section, we analyze the ability of a fan beam and a dual synchronous system to image in clear ocean water small mid-water nekton and to determine the limitations of such a system.

II ANALYSIS OF FAN BEAM IMAGING IN SEA WATER

A. Introduction

The problem we are addressing is to determine the requisite spatial resolution as a function of contrast of the object and the detector signal-to-noise ratio of a viewing system whose sensor is a self-scanned imaging array of detectors and whose illuminating source is a scanning fan beam. In this analysis, it is assumed that the field-of-view (FOV) is fixed. The use of a fixed FOV is not a necessary restriction; however, if the results indicate that it is responsive to the requisite requirements for nekton viewing, it would simplify the fabrication of such a system.

The system geometry is indicated in Figure 2. Here, a fan beam of light (i.e. laser or non-laser) of fan angle $2\beta_F$ is directed such that the fan angle covers the vertical FOV of the detector system at a given time. As the fan beam scans in the horizontal direction, it covers the fixed FOV of the detector system.

At any given instant, the fan beam at the range R will be dispersed due to particulate scattering and attenuated due to particles and dissolved materials in the water. As a result, the resultant angular intensity of the beam at a given range depends on the water scattering and attenuation properties in addition to the range.

For a viewing system that is to perform beyond an attenuation length, it is necessary to take into account multiple scattering. Due to the fact that there is no satisfactory expression in closed form that describes this process, we utilize the theory of MTF for analyzing the foward scattering process. As our ultimate goal is angular resolution, MTF theory (modulation transfer function) provides a means for determining this process in closed form, knowing

the volume scattering function, $\sigma(\theta)$, valid for single scattering only and the attentuation coefficient of the sea water.

B. Derivation of the Transfer Equations

In order to use MTF theory, it is necessary to know the response of the system to a point source (impluse response in electronics or Green's function in mathematics). The point source will produce, after passing through the system, a point spread function, $S(\theta)$, which characterizes how a point source of light is dispersed spatially on the observation plane. As the fan beam can be considered to made up of many point sources, the resultant distribution becomes a summation process.

The situation is depicted in figure 3. We use angular coordinates rather than spatial coordinates due to the dependence of the results on range. The θ_x and θ_y axis represent the coordinate axis of the target plane. It is found that referring all results to the target plane simplifies the analysis. The coordinates indicated in parenthesis are dummy variables used for the integration.

Consider the fan beam in an ideal medium at the range R. At the target plane, the fan beam can be represented mathematically as a rectangle function (Rect) in the ε direction and a delta (δ) in the η direction. In the η direction we assume that diffraction effects are negligible and that the spatial dispersion is caused only by the sea water scattering. In addition, we assume that the point spread function is known, $S_p(\theta_x, \theta_y)$, as we describe later how this function is derived from the scattering, and attentuation coefficients. If at a given time, the fan beam is located at say η_o, then the fan beam can be written as Rect(ε) $\delta(\eta)$ where $|\varepsilon| \leq \beta_F$. A point in the fan beam is dispersed bt $S_p(\theta_x, \theta_y)$ and hence is written

as $S_p(\theta_x - \eta, \theta_y - \varepsilon)$, (i.e. the S_p is displaced to η, ε). Consequently, the resultant angular dispersion of the fan beam is the summation of the displaced spread function over the length of the fan beam. This can be written as,

$$S_L(\theta_x,\theta_y,R) = \iint_{-\infty}^{\infty} S_p(\theta_x-\eta, \theta_y-\varepsilon, R)\,\mathrm{Rect}(\varepsilon)\,\delta(\eta-\eta_o)\,d\eta\,d\varepsilon \quad (1)$$

where, S_L now represents the line spread function of the fan beam located at η_o. Integrating out the η, we have that,

$$S_L(\theta_x-\eta_o,\theta_y,R) = \int_{-\beta_F}^{\beta_F} S_p(\theta_x-\eta_o,\theta_y-\varepsilon,R)\,\mathrm{Rect}(\varepsilon)\,d\varepsilon \quad (2)$$

As equation (2) is a one demensional convolution, we have from Fourier Transform theory that,

$$\tilde{S}_L = \tilde{S}_p \frac{\sin \omega_{\theta y} \beta_F/2}{\omega_{\theta y} \beta_F/2} \quad (3)$$

where, $\omega_{\theta y}$ is the conjugate angular variable to θ_y (i.e. radians of spatial frequency/ radians of angle) and the $\sim$ symbol means the transform of. This expression will be utilized later in the derivation. As can be seen that if the S_p is known in closed form, the resultant resolution due to the fan beam can be determined in frequency space.

Expression (2) represents an irradiance function. It is now necessary to consider how this irradiance reflecting off of a target is viewed by the imaging system. A lens looking at a point on this distribution sees a blur given again by S_p. In this derivation, it is assumed that the difference in the range R from the illuminator

to the target and from the viewing system to the target is negligible. As before, each point on the target plane is viewed as a blur and the resulting intensity distribution is a summation of this blur over the irradiance of the object. Consequently,

$$I(\theta_x, \theta_y) = \int_{-\infty}^{\infty}\int S_p(\theta_x-\eta, \theta_y-\varepsilon, R) S_L(\theta_x-\eta_o, \theta_y, R)\rho(\eta,\varepsilon)\,d\eta\,d\varepsilon \quad (4)$$

where, $\rho(\eta, \varepsilon)$ represents the target reflectivity and I (θ_x, θ_y) represents the apparent intensity as viewed by the detector system at the angular coordinates (θ_x, θ_y). As before, equation (4) represents a convolution of S_p with $S_L\rho$. Consequently, in the frequency domain, equation (4) can be written as,

$$\tilde{I} = \tilde{S_p} \cdot \widetilde{S_L\rho} \quad (5)$$

However $\widetilde{S_L\rho} = \tilde{S}_L \otimes \tilde{\rho}$ where $\otimes$ stands for convolution. Substituting from equation (3) we have that,

$$\tilde{I} = \tilde{S_p} \cdot \tilde{S}_L \otimes \tilde{\rho} = \tilde{S_p} \cdot \tilde{S_p} \frac{\sin \omega_{\theta y} \beta_F/2}{\omega_{\theta y} \beta_F/2} \otimes \tilde{\rho} \quad (6)$$

It is interesting to note that if the η_o of S_L were also a variable (i.e. broader beam illumination), equation (6) would read,

$$\tilde{I} = \tilde{S_p} \otimes \tilde{S}_L \cdot \tilde{\rho} = \tilde{S_p} \otimes \tilde{S_p} \frac{\sin \omega_{\theta y} \beta_F/2}{\omega_{\theta y} \beta_F/2} \cdot \tilde{\rho} \quad (7)$$

Comparing (6) with (7) we see that in a broader beam illumination, resolution can be derived from the illuminator and detector as a convolution in frequency space means a greater resolution. In the case of the fan beam, the product $\tilde{S}_p \cdot \tilde{S}_L$ represents less resolution

while convolution with $\tilde{\rho}$ represents greater or less resolution depending on the frequency content of $\tilde{\rho}$.

In any event, equation (6) is the basic equation that will be used for subsequent calculations and represents the imaging ability of the entire system at a given position of the fan beam.

C. The Point Spread Function

In order to utilize equation (6), we require an expression for S_p or more explicitly, $\tilde{S}_p$. It has been shown by Wells[2] that the transform of the point spread function can be written as,

$$\tilde{S}_p = e^{-D(\nu)R} \tag{8}$$

where,

ν = spatial frequency (cycles/radian)

$D(\nu) = \alpha - \int_0^{\cdot} \widetilde{\sigma(\theta t)}\, dt$ (frequency decay function)

with,

$\sigma(\theta)$ = volume scattering function

α = attentuation coefficient

Here, $\widetilde{\sigma(\theta)}$ is expressed as the Fourier-Bessel transform of $\sigma(\theta)$ and is written as,

$$\widetilde{\sigma(\theta)} = 2\pi \int_0^{\epsilon} J_0(\omega\theta)\sigma(\theta)\theta\, d\theta \tag{9}$$

where, $J_0(\omega\theta)$ is the zero order Bessel function and ϵ represents the dividing angle between small and large angle scattering. The calculation of $D(\nu)$ requires an analytical expression for $\sigma(\theta)$. Wells has proposed the following as an adequate expression for the foward scattering,

$$\sigma(\theta) = \frac{s\,\theta_o}{2\pi\left[\theta_o^2 + \theta^2\right]^{3/2}} \qquad (10)$$

where, s and θ_o are adjustable parameters and s is given by,

$$s = \alpha - \gamma = 2\pi \int_o^{\epsilon} \sigma(\theta)\,\theta\,d\theta \qquad (11)$$

with γ = broad beam attentuation coefficient (i.e. γ represents the fraction of light scattered out of a cone of light, taken usually as 10^o) while s represents the fraction of light within the cone. Consequently, a given θ_o and α defines D(ν) which in turn defines $\widetilde{S}_p$.

D. Normalization

In above derivations, no attempt was made to normalize the resulting equations. This can be done by noting that the S(θ ,R) is defined as the fraction of power at the range R per unit solid angle (Ω). If we assume that most of the scattering is contained in the forward direction (i.e. large particles of radius $>1\,\mu$), then,

$$\int_o^{\Omega_{MAX}} S_L\,d\Omega \cong P_o \qquad (12)$$

with P_o the total power in the beam, Consequently, $P_o\,S_L(\theta, R)$ represents the fraction of power falling on the target at R per unit solid angle. If we assume unit reflectivity of a Lambertian target, then the reflected radiation from the target is $P_o S_L/\pi$. A detector system viewing this target has an angular area of its resolution element of $\pi\epsilon_t^2$ where ϵ_t represents the angular radius.

The collector lens views each radiating point with a solid angle of A_D/R^2 where A_D is the collection area. As viewed by the detector, the normalized return is just $P_o \in_t{}^2 A_{D/R^2}$. This represents the fraction of power received by a given resolution element in the detector system. Utilizing short hand notation, equation (4) can be written as,

$$I(\theta)_{RES.\ ELEM.} = \frac{P_o \epsilon_t^2 A_D}{R^2}\left[S_p(\theta) \otimes S_L(\theta_x - \eta_o, R)\rho(\eta,\varepsilon)\right] \quad (13)$$

In terms of received photons necessary for the noise calculations below, we have that,

$$\Phi_s(\theta_x,\theta_y) = \frac{N\phi P_o \epsilon_t^2 A_D t}{R^2}\left\{S_p(\theta) \otimes S_L(\theta)\rho(\eta,\varepsilon)\right\} \quad (14)$$

where,, $N\phi$ = number of photons /joule and t = integration time. Equation (14) transformed reads,

$$\widetilde{\Phi}_s(\nu_x,\nu_y,R,\eta_o) = \frac{N\phi P_o \epsilon_t^2 A_D t}{R^2}\left\{\widetilde{S_p}\cdot\widetilde{S_L} \otimes \widetilde{\rho}\right\} \quad (15)$$

Equation (15) represents the signal per unit frequency interval received by the detector having a resolution of ϵ_t looking at the coordinates θ_x, θ_y at the range R with the fan located at η_o.

E. Background, Signal-To-Noise Ratio and Contrast

As equation (15) represents the signal, it is necessary to calculate the expected background due to backscattering from the beam into the FOV of the detector. We will assume that the projected fan beam dispersed by the sea water will look like an elliptical cylinder (figure 4). The viewing system looking at an resolution element in

the middle of the cyclinder "sees" a column of scattered light determined by the angle between the beam and detector axis. The maximum scattering occurs at the center of the cylinder as this point has the widest angular spread. The relationship between the angle of viewing and the radial spread ($\theta_{max}^{R)}$ (containing most of the energy) can be written as,

$$r \cong \frac{2\,\theta_{MAX}\,R}{\tan \gamma} \tag{16}$$

where, r is the distance through which a resolution element is viewed and γ is the viewing angle with θ_{max} about 10^{o}. The backscattering can be characterized by the backscattering coefficient $\sigma_{B}(180^{o})$ which has units of fraction scattered per unit length per unit solid angle. Hence, $\sigma_{B} r$ is the diffuse reflectivity in the backward direction (toward the viewing system). This derivation assumes that the σ_{B} does not vary much over a wide arc at 180^{o}. As the angular spread is determined by the S_{L} and it is viewed as a blur determined by S_{p}, the resultant background, analogous to equation (15), is,

$$\phi_{B} \cong \frac{N_{\phi} P_{o} \epsilon_{t}^{2} A_{D} t \pi \sigma_{B} r}{R^{2}} \left\{ \tilde{S}_{p} \cdot \hat{S}_{L} \right\} \tag{17}$$

In order to relate the signal-to-noise ratio (SNR) of the detector with the medium and target transform, we proceed as follows:
The receiver contrast in terms of SNR can be written as,

$$C_{R} = \frac{SNR}{\sqrt{S+B}} \tag{18}$$

With the SNR fixed, the receiver contrast can be computed from

equations (15) and (17). Comparing (15) and (17) we note that the signal S can be written as $S = \Phi_S' \in_t^2$ and the background $B = \Phi_B' \in_t^2$. Substituting in (18) we have that,

$$C_R = \frac{SNR}{\epsilon_t \sqrt{\Phi_S' + \Phi_B'}} \tag{19}$$

Equation (19) indicates that the smaller the resolution required, the higher the contrast must be to meet the SNR requirement. Using the Rayleigh criterion for resolution, we have that,

$$2\pi \epsilon_t \nu = 1.22\pi \tag{20}$$

and hence $1/\epsilon_t \approx 1.6$. As a result we have that,

$$C_R \approx \frac{\nu \cdot SNR}{\sqrt{\Phi_S' + \Phi_B'}} \tag{21}$$

Equation (21) relates the spatial frequency to the detector contrast and the SNR. Note that the C_R is directly proportional to ν contrary to the MTF of the medium-target system. The MTF of the combined system was derived above as,

$$C_{MT}(\nu) = \widetilde{S_P} \cdot \widetilde{S_L} \otimes \widetilde{\rho} \tag{22}$$

normalized to $\nu = 0$.

Finally, we equate (21) to (22) to satisfy both detector and system requirements as,

$$\tilde{S}_p \cdot \tilde{S}_L \otimes \tilde{\rho} = \frac{\nu \, SNR}{\sqrt{\Phi_S' + \Phi_B'}} \qquad (23)$$

A seperate plot of each side of the equation will produce a crossing point at some ν_o which is the maximum resolution of the entire system.

F. Evaluation of the Contrast Functions

As a starting point we have chosen those parameters that are characteristic of clear ocean water starting at about 500 meters in depth. The parameters that chracterize the water are α, the attentuation coefficient; s_T, the total scattering coefficient; s, the scattering coefficient for a broad beam and θ_o, a parameter that characterizes the volume scattering function along with a (see equation (10). The parameters we have chosen were taken from the work of D. Matlack[3] in which the attenuation coefficient measurements and scattering at 15^o and 33^o were made down to about 5000 meters for several ocean areas. From a typical deep ocean enviroment we chose the following parameters:

α = .05 meter^{-1}

s_T = .005 meter^{-1} (based on 15^o and 33^o scattering data)

s = .0025 meter^{-1} steradian^{-1} (estimated)

θ_o = .15 radians (based on fitting

These parameters represent the scattering and attentuation properties at about 432 nm.

Before proceeding, it is necessary to evaluate $\tilde{s}_p x \, \tilde{s}_L$. This factor appears in all of the relevant transmission equations derived. We call this factor τ, which represents the imaging characteristics.

of the ocean/fan beam combination. Hence we write,

$$\tilde{S}_p \cdot \tilde{S}_L = \tau(\omega, \phi) = e^{-D(\omega)R} \cdot e^{-D(\omega)R} \frac{\sin(\omega_y \sin\phi \beta_F/2)}{\omega \sin\phi \beta_F/2} \quad (24)$$

or,

$$\tilde{S}_p \cdot \tilde{S}_L = \tau(\omega, \phi) = e^{-2D(\omega)R} \frac{\sin(\omega \sin\phi \beta_F/2)}{\omega \sin\phi \beta_F/2} \quad (25)$$

It has been shown by Wells[2], that $D(\omega)$ can be written as,

$$D(\omega) = \alpha - \frac{s[1 - e^{-\omega\theta_0}]}{\omega\theta_0} \quad (26)$$

Substituting we have that,

$$\tau(\omega, \phi) = e^{-2\alpha R} \cdot e^{\frac{2sR[1-e^{-\omega\theta_0}]}{\omega\theta_0}} \cdot \frac{\sin[\omega \sin\phi \beta_F/2]}{\omega \sin\phi \beta_F/2} \quad (27)$$

In order to compute the expected resolution for the sea/light source system as expressed in equation (22), we now evaluate, for a range of 100 meters.

$$\tilde{S}_p \cdot \tilde{S}_L \otimes \tilde{\rho} = \tau(\omega) \otimes \tilde{\rho}(\omega) \quad (28)$$

It is to be noted that the convolution expressed by (28) is only in the ω_y direction. As a result, we have,

$$C_{MT}(\omega) = e^{-10} \cdot e^{\frac{.5(1-e^{-.15\omega_y})}{.15\omega_y}} \cdot \frac{\sin .17\omega_y}{.17\omega_y} \otimes \tilde{\rho}(\omega_y) \quad (29)$$

The factor sine .17 ωy/ .17ωy has its first zero at .17 $\omega_y = \pi$ or 2 π (.17) ν_y = π . Hence ν_y = 1/.34 $\cong$ 3 cycles/radian. As the secondary zeros of the sine function are much lower in magnitude, we can approximate the sine function by an one demensional delta function (i.e. it has the effect of reproducing the $\tilde{\rho}(\omega_y)$ without modification). In addition, the $\tilde{\rho}(\omega_x)$ represents the sampling of the $\tilde{\rho}(\omega_x)$ at some frequency component. With these modifications we can write that,

$$C_{MT}(\omega) = e^{-10} \cdot e^{\frac{.5(1-e^{-.15\omega})}{.15\omega}} \cdot \tilde{\rho}_s(\omega_x) \cdot \tilde{\rho}(\omega_y) \tag{30}$$

where $\tilde{\rho}_s(\omega_x)$ means the sampled value of the x component of $\tilde{\rho}$ (ω). It is also noted that the expression 1 - $e^{-.15\omega}$/.15ω goes to 1 as ω goes to zero. Hence at ω_y = 0, we have that,

$$C_{MT}(0) = e^{-9} \tilde{\rho}_s(\omega_x) \cdot \tilde{\rho}(0) \tag{31}$$

As ω goes to ∞ , C_{MT} becomes,

$$C_{MT}(\infty) = e^{-10} \tilde{\rho}_s(\omega_x) \cdot \tilde{\rho}_y(\infty) \tag{32}$$

This indicates that the contrast goes from a peak of e^{-9} to e^{-10}. Before proceeding, it is now necessary to consider the ramifications of sampling in the θ_x direction.

G. Sampling Theory

The fan beam at each position in effect samples the image content in the θ_x direction. This can be described mathematically by considering that the image to be reconstructed is sampled by an array

of delta (δ) functions in the θ_x direction. This can be written as,

$$\mathrm{comb}\left(\frac{\theta_x}{\theta_{x_o}}\right) = \sum_{n=-\infty}^{\infty} \delta\left(\theta_x - n\theta_{x_o}\right) \tag{33}$$

where θ_x is the continous variable and the θ_{x_o} is the sampled positions. Hence we can write,

$$\rho_s(\theta_x) = \mathrm{comb}\left(\frac{\theta_x}{\theta_{x_o}}\right)\rho(\theta_x) \tag{34}$$

where $\rho_s(\theta_x)$ represents sampled reflectivities along θ_x. If we make the assumption that the ρ is bandlimited (i.e. limiting the highest frequency component to be resolved), then it can be shown that [4],

$$\tilde{\rho}_s(\omega_x) = \sum_{n=-\infty}^{\infty} \tilde{\rho}\left[\omega_x - \frac{2\pi n}{\theta_{x_o}}\right] \tag{35}$$

This means that the spectrum of $\rho_s(\theta_x)$ can be found by erecting the true spectrum of $\rho(\theta_x)$ about each point (n/θ_{x_o}) in the ω_x direction. As the ρ is assumed to be bandlimited, its spectrum $\tilde{\rho}$ is nonzero over only a finite region of frequency space. It can also be shown that in order to recover the image exactly, (within the bandlimited assumption), then it is necessary to have,

$$\theta_x \leq \frac{1}{2B_x} \tag{36}$$

where B_x represents the highest frequency component to be recovered. It is our intention to attempt to "recognize" rather than to recover the image exactly. As a result, less sampling points are required and places less restrictions on the data transmission system. The

more we relax the B_x of (36), the less sampling points are required.

If we have only one sampling point, (i.e. the fan beam at one location), then aliasing occurs- false information is retrieved- in the θ_x direction and we have little or no information about the ω_x due to the complete overlapping of the individual spectrums of $\tilde{\rho}(\omega_x)$. As we increase the number of sampling points, the individual spectrums move apart in frequency space until there is no overlap. At this point, complete image recovery can be obtained by injecting at each sampling point (artificially) an interpolation function given by,

$$\frac{\sin\left[2B_x(\theta_x - n/2B_x\right]}{2B_x(\theta_x - n/2B_x)} \qquad (37)$$

We will assume that the $\tilde{\rho}_s(\omega_x)$ is a constant term equal to one and proceed to calculate the expected resolution in the θ_y direction.

H. Calculation of the Expected Resolution

Returning to equation (32) with $\omega_x = 0$, we write that,

$$C_{MT} = e^{-9.5} \cdot \frac{e^{.5(1-e^{-.15\omega})}}{.16\omega} \tilde{\rho}(\omega_y) \qquad (38)$$

In order to relate this to the detector contrast requirements, we note that (see equation (15) and (22)),

$$\tilde{\Phi}_s' = \frac{N\Phi P_o A_D t}{R^2} \cdot C_{MT} \qquad (39)$$

and that,

$$\tilde{\Phi}_B' = \frac{N\Phi P_o A_D t \pi \sigma_B r}{R^2} \cdot \tau \qquad (40)$$

Now from equation (21),

$$C_R \cong \frac{\nu \cdot SNR}{\sqrt{\Phi_S' + \Phi_B'}} \tag{41}$$

or,

$$C_R \approx \frac{R\nu_y \cdot SNR}{\sqrt{N_\Phi P_o A_D t} \cdot \sqrt{C_{MT} + \pi \sigma_B r \tau}} \tag{42}$$

For σ_B we use the value for clean water ($\sim 3\times10^{-4}$ $m^{-1}ster.^{-1}$) and the r is calculated from equation (16) for $\tan \gamma = 45^o$ and $\theta_{max} = 10^o$ with R = 100 meters. Hence r = 35 meters and,

$$C_R \approx \frac{100\nu_y \cdot SNR}{\sqrt{N_\Phi P_o A_D t} \cdot \sqrt{C_{MT} + .03\tau}} \tag{43}$$

The factor $\sqrt{N\ P_o A_D t}$ we call Q, a pseudo figure of merit. Hence,

$$C_R \approx \frac{100\nu_y \cdot SNR}{Q\sqrt{C_{MT} + .03\tau}} \tag{44}$$

If the fan beam wavelength is taken at 432 nm, then $N_\Phi \cong 2.2\times10^{18}$ photons/joule. If a typical power is 1 watt and A_D is taken as about .01 $meter^2$ with an interrogation time of 10^{-3} sec., a typical Q would be about 4.7×10^6. Thus we write that,

$$C_R \approx \frac{2\times10^{-5} SNR \cdot \nu_y}{\sqrt{C_{MT} + .03\tau}} \tag{45}$$

For values of $\nu_y > 3$ cycles/radian, $\tau \cong 0$. Then,

$$C_R \approx \frac{2 \times 10^{-5}\, SNR \cdot \nu_y}{\sqrt{C_{MT}}} \tag{46}$$

For large values of ν_y, $C_{MT} = e^{-9.5}\,\tilde{\rho}(\omega_y)$. In order to set some limit on $\tilde{\rho}(\omega_y)$, we will assume that lower limit is .05. Hence,

$$C_R \approx 10^{-2} SNR \cdot \nu_y \tag{47}$$

As a limiting case, for SNR = 1, then,

$$C_R \approx 10^{-2} \nu_y \tag{48}$$

If the $\tilde{\rho}(\omega_y)$ had been set to 1, then,

$$C_R \approx 2.5 \times 10^{-3} \nu_y \tag{49}$$

In order to compare this equation (38), we equate the normalized $C_{MT}(\omega_y = 0)$ to C_R. A plot of equation (49) and normalized equation (38) is shown in figure 1. As indicated in figure 5, the resolution is determined by the object contrast ratio (i.e. nekton) and the detector requirements and not by the sea water. For this case (upper limit), the spatial angular frequency occurs at about 61 cycles/ radian times the frequency contrast ratio of the nekton. Since $\nu_y \cong 1/\theta_y$, then $\theta_y \cong$ 16 milliradians at 100 meters. This corresponds to a spatial resolution of about 1.6 meters.

I. Conclusions

It is expected that for nekton of low contrast, resolution is poor and only nekton with high contrast markings (i.e. striped, colored etc.) can be expected to give decent resolution. It is to be noted that the contrast requirements for the detector goes directly as R. A corresponding calculation at 50 meters would effectively increase the resolution to 40 centimeters (8×10^{-3} radians x 50 meters).

Additionally, resolution can be increased by increasing the interrogation time and hence increasing the Q value. If the interrogation time is increased to 10 milliseconds, then the C_R requirements are reduced to 1/3 of the value at 1 millisecond. Consequently, the resolution is increased to about 13 centimeters at 50 meters. Since the value of A_D that is used to calculate Q is limited, the only variables that affect the Q are P_o and t. Limitations on available power and interrogation time requirements for data transmission will ultimately set the upper limits of resolution.

Because of the great variability of nekton markings and shape, exact calculations of resolution expected are quite academic. We require a criterion that can be used to indicate what constitutes a count (i.e. if the system is to be used to measure nekton populations). The magnitude of the problem is enormous and in the short study we can only indicate the direction that any future study should take.

It is our belief that exact imaging is much too limited to be useful as a counting tool and hence we will depend on pattern recognition as a possible method to circumvent some of the difficulties presented. This means that classes of nekton (not species) must be categorized enough so that by sufficient sampling it can be recognized as such.

III. ANALYSIS OF SHORT RANGE IMAGING REQUIREMENTS

A. General Requirements

As mentioned in section II, the variety of the nekton presents an enormous characterization problem. In order to make the analysis somewhat tractable, we have chosen two particular classes of nekton for the analysis. The rationale for choosing these two classes of nekton stems from the belief (partially supported by experimental observations) that the sea's deep scattering layer (DSSL) is predominantly due to (1) myctophids or lantern fish and (2) shrimp-like crustaceans called euphausiids and sergestids[5]. Nets towed at night at the surface of the ocean pick up one to five of these individuals per cubic yard and as many as 20 per cubic yard.

Representatives of these two classes of nekton are shown in figure 6. These animals vary in length from one inch to three inches. Characterization of the myctophids is tabulated in appendix A. Both of these animals have luminescent spots on their bodies called photophores. This liminescence has been correlated with the diurnal movement of the DSSL and the intensity has been measured to be about 5×10^{-4} microwatts per square centimeter at 474 nm.

If the design goals of a nekton viewing system is to produce a system that has an effective opening of 1000 meter^2 combined with good spatial resolution, then even for a recognition system, the problem is a formidable one.

B. Reassessment of Viewing Design

Based on the analysis of section II it was found that even for high contrast nekton markings at 100 meters, the expected resolution is on the order of 25 cm. As we are dealing with animals with sizes on the order of 2 to 7 cms. in length, recognition is not possible even with sampling techniques. Consequently, we are forced to

reassess the viewing configuration originally considered in order to produce a system that can be used as a counting tool with the requisite requirements.

If we use a criterion that at least 10 sampling points are necessary to recognize crustaceans (i.e. about 2mm resolution) and that we require an effective mouth opening (viewing area) of about 1000 meter^2, then we are forced to consider a short range beam used in some circular fashion to produce the requisite viewing area.

If a system can be devised that meets these two requirements, then the system will automatically be suitable for the larger nekton responsible for the DSSL. Each requirement will be examined below.

C. Resolution Analysis

Based on the contrast requirements described in section II we found that the limitation on contrast was due to the detector requirements and not the sea-water. As we are now considering shorter ranges (on the order of 20 meters), we can neglect the sea-water scattering using the values stated in sectionII. This can be seen from the fact that s_T = .005 meter^{-1}. With a round trip distance of 40 meters, the total scattered energy from the beam is $e^{-.2}$ or about 18%. As this is the total scattering, it is expected that less than 10% is in the foward direction. As a result, the imaging equations can be simplified considerably from the ones given in section II.

Again considering a fan beam with a fan angle of about 20^o (.35 radians)the total power in the beam, P_o , is spread out into a rectangle of negligible width (about 1 cm,) and a length of .35R. Then the power density at the distance R is about 286 P_o/R (watts/ meter^2). If we assume a uniform attenuation (using an α = .05 meter^{-1}), then,

$$P' = \frac{P}{M^2} = \frac{e^{-.05R}\, 286\, P_o}{R} \tag{50}$$

Consequently, this represents the irradiance function similar to equation (3). Equation (50) becomes the radiance function when divided by π and multiplied by the area over which reflection takes place, then,

$$\frac{P'}{\Omega} = B = 286\, e^{-.05R} P_o R \epsilon^2 \rho(\epsilon) \tag{51}$$

where,

ϵ = angular radius of reflective resolution element
$\rho(\epsilon)$ = reflectivity from region of angular radius
Ω = solid angle

The corresponding background radiance is similarly given by,

$$B_B = 286\, e^{-.05R} P_o R \epsilon^2 \rho_B(\epsilon) \tag{52}$$

However, from section II, the ρ_B can be written as,

$$\rho_B = \pi \sigma_B r \tag{53}$$

where,

σ_B = the backscattering coefficient
r = effective distance through which the resolution element is viewed

In travelling the distance to the detector, both the B and B_B are further attentuated by $e^{-.05}$ (here we assume that the target-source distance and detector distance are the same). The effective signal received by the detector system per resolution element is just,

$$S = \frac{B A_D t e^{-.05}}{R^2} \tag{54}$$

where,

A_D= area of collecting optics
t = integration time

and also that,

$$B = \frac{B_B A_D t e^{-.05}}{R^2} \tag{55}$$

The signal to background radiance ratio becomes just,

$$\frac{S}{B} = \frac{\rho}{\pi \sigma_B r} \tag{56}$$

For typical clean water with a value of σ_B about 3×10^{-4} meter^{-1} steradian^{-1} and a value of r on the order of a few cms., $\pi \sigma_B r$ is about 10^{-5}. Consequently, we can neglect the background radiance for values of ρ greater than .01. Hence, we can write that the incoming signal per resolution element of the object is,

$$S = \frac{286 e^{-.1R} P_o R \epsilon^2 \rho A_D t}{R^2} \tag{57}$$

or,

$$S = \frac{286 e^{-.1R} P_o \epsilon^2 \rho A_D t}{R} \tag{58}$$

If we call $P_o A_D t$, M, a figure of merit, then,

$$S = 286 \left(\frac{e^{-.1R}}{R}\right) \rho \epsilon^2 M \tag{59}$$

For P_o = 1 watt, A_D = .01 meter^2 and t = 10 milliseconds, then,

$$S \cong .03 \left(\frac{e^{-.1R}}{R}\right) \rho \epsilon^2 \text{ (JOULES)} \qquad (60)$$

For a typical photodiode array, the leakage current is on the order of 1/3% of the saturation value for a line scanning time of 10 milliseconds[6]. A typical saturation value is about 1 microjoule/cm^2 or about 10^{-9} joules/resolution element. As a result, for a signal to noise ratio of 1, the signal required for detection is on the order of 3×10^{-12} joules/resolution element. Hence equation (60) becomes,

$$\rho \epsilon^2 = 10^{-10} R e^{.1R} \qquad (61)$$

This indicates that the detection depends on the product of reflectivity and angular resolution squared. A plot of $\rho\epsilon^2$ against R is shown in figure 7. The corresponding value of ϵ for a given ρ can be read off the curve of figure 8. For example, at 17.5 meters, $\rho\epsilon^2 = 10^{-8}$ from figure 7. For a ρ = 0.1, the $\epsilon = 3.2 \times 10^{-4}$ radians or a spatial resolution of 1 cm. At ρ = 1.0, the corresponding resolution would be .3 cm. Hence, the curves of figures 7 & 8 can be used to predict the short range spatial resolution for a given ρ and R. It is noted in passing that this derivation was based on negligible scattering and is valid for a range of a few attenuation lengths. Further, it is noted that the curves are for a S/N of 1 and good recognition would require a higher S/N. In addition, as it was assumed that the fan beam width remains constant throughout the range at 1 cm., the maximum resolution of interest is $\epsilon = 2 \times 10^{-4}$ radians at 20 meters or a spatial resolution of about 4 mm in object space.

D. Recognition Requirements

The preceeding analysis indicates that for the fan beam under consideration, we must limit the range to something on the order of 20 meters with an angular resolution of 2×10^{-4} radians or better.

If we are required to recognize the small crustaceans (about 2 cm.) in designing a viewing system, then we must establish the minimum resolution necessary for recognition.

As recognition of an object is a trained subjective response, it becomes difficult to state quantitively what constitutes recognition. In addition, the constraint of producing a large sampling area runs counter to the resolution requirements. The information necessary for proper recognition is less if a human observer is used than if a computer is used. However, to obtain some idea of what can be recognized, we will assume that an object can be recognized as such if we sample at least 10 areas of the object along any demension (i.e. the object is to be reconstructed from only 10 resolution elements). This corresponds to at least 2mm resolution for the smallest crustacean. In terms of ϵ , this will range from 10^{-4} radians for 10 meters to 5×10^{-5} radians for 20 meters. For 10 meters, $\rho\epsilon^2$ (figure 7) is about 3×10^{-9}. Hence, ρ must be .3 or greater for recognition. For 20 meters, $\rho\epsilon^2$ is 1.5×10^{-8} or ρ must be 6.0 or greater which is not physically possible. At 15 meters, the values are $\rho\epsilon^2$ equal to 6×10^{-9} with ϵ equal to 6.67×10^{-5} from which ρ must be 1.50 or greater which is also not physically possible. Hence, we conclude that for proper recognition of 2cm. crustaceans, the range must be limited to about 14 meters for unit reflectivity. As it is believed that the reflectivity is on the order of 50 %, this further restricts the range to about 12 meters.

In order to satisfy the requirement of large sampling area, this would

suggest that the only way to achieve this is to have a circular scan arrangement with a radius of 12 meters producing an effective sampling area of about 400 meters^2. This does not meet the desirability of a sampling area of 1000 meters^2 as it is limited by the size of the crustaceans to be recognized, their reflectivity and the detector requirements.

E. Suggested Scanning Arrangement

Based on the above analysis, it is suggested that a fan beam of about 20^o angle be used coming from the tip of the towed fish using fiber optics for the coupling. The fan beam can be stepped every 10 millisecond. A total time of 90 milliseconds would result for a complete circular scan. In addition, if the towed fish is moving at 1 knot (½ meter/sec.), then the circular fan beam is effectively sampling every 5 cm. The width of the beam could be doubled to compensate partially for this with a loss of power density of a factor of 2. The looking time could be decreased to 5 milliseconds so that the sampling overlaps slightly during each revolution. The system is depicted diagramatically in figure 9. The viewing system would have to move synchronously with the stepping fan beam. With such a system, the sampled volume would be about 200 meter^3/sec. Based on our previous report on the expected density of fish (10/meter^3), this would correspond to about 2000 counts/sec.

In section IV, we examine some of the myctophid characteristics that might be suitable parameters for pattern recognition.

blank

IV. GEOMETRIC AND BIOLUMINESCENT CHARACTERIZATION OF MYCTOPHIDS

A. Statement of the Problem

In the previous two sections we have established the following as necessary for a viable deep water imaging system for counting nekton:

1. The electro-optical system is to be used to count nekton of grossly different morphology only (i.e. no differentiation of species)
2. The euphasiids and the myctophids represent the lower limit of the imaging system in terms of size and reflectivity
3. The imaging system must operate at relatively close range- on the order of 20 meters- in order to properly image the nekton of 2
4. In order to acheive the largest possible sampling volume, the illuminating beam should be used in some circular fashion

In addition to these constraints, it is also necessary for any viewing system to be able to recognize and count the variety of the nekton present. Consequently, a viable system must incorporate a pattern recognition hierarchy capable of sorting and counting in real time the changing images presented to the system. The necessity for such a pattern recognition system cannot be overemphasized as the following illustrates.

A typical school of myctophids may have a thickness of 10 meters with a diameter of 50 meters. With a myctophid density of about 10/ meter^3, the school represents about 200,000 myctophids. Assuming that the viewing system is travelling parallel to the diameter of the school at ½ meter/sec. (about 1 knot), it would take the viewing system about 100 sec. to traverse the school of myctophids.

The system must be capable of counting and recognizing myctophids at the rate of 2000/sec. This is an enormous task unless the system is programmed to recognize and count in a prescribed manner.

As the nekton at rest are normally horizontal or slightly oblique but in any orientation, the pattern recognition hierarchy must be able to recognize the prescribed shapes and sizes in any orientation. This problem is an order of magnitude more difficult to accomplish than the pattern recognition techniques used presently in microscopic image analysis where all objects to be recognized are restricted to a plane.

It is noted in passing, that the pattern recognition hierarchy is necessary whether acoustic or optical imaging imaging is used.

B. Characterization of the Myctophid Family by Size and Shape

Using the myctophid family of nekton as a model (lantern fish), we wish to develop a unique characterization that can be recognized by a suitable optical/computer system. We consider the following parameters as a means of developing a geometric characterization of these nekton:

1) Length: 3.5 to 13 cm.
2) Shape:
   a. Side on: fusiform (spindle shaped at both ends)
   b. End on: flat-sided flanks (ellipsoidal cross-section)
3) Speed: 10 cm/sec. maximum (sluggish swimmers)
4) Vision: maximum absorption about 480 nanometers
5) Bioluluminescence: characteristics to be described in C below
6) Area: app. $.1L^2$ (described below)
7) Pseudovolume: reflectivity times area
8) Perimeter: app. 2.1L (described below)

The characterization we are attempting to develop must be able to

distinguish the myctophid family of nekton found in the mesopelagic zone. We are only considering for this work side-on views in any orientation. The more difficult problem of "in depth" orientation will be pursued at a later time.

The model we are using for characterization is shown in figure 10. Due to the silvery sides of this nekton, an imaging system will probably not be able to distinguish the fins or tail (due to difference in reflectivity). Consequently, the image presented to the computer system will be one of uniform intensity outlined against nearly black water. As a first cut, we section the lantern fish as indicated in figure 11. The numbers are cast in terms of its length. From this model we arrive at the following parameters compared to a uniform circle of diameter L, of unit reflectivity and a line of length L of unit reflectivity.

	Line (R=1)	Uniform Circle (R=1)	Myctophid
P(Perimeter)	app. 2L	3.14L	app. 2.1L
A(Area)	δ xL	app. $.8L^2$	app. $.1L^2$
V(Pseudovolume)	δ xL	app. $.8L^2$	app. $Rx.1L^2$

where δ = delta function of thickness approaching zero

As can be seen, the perimeter has a range of 2L to πL; the area a range of δL to $.8L^2$ and the pseudovolume a range of δ L to $.8L^2$. No single parameter is useful for characterization as many mesopelagic nekton have parameters not too different from the myctophids.

If we examine non-demensional combinations of the above parameters, we have shape information from P^2/A and density information from A/V.

	Line	Myctophids	Circle
Shape (P^2/A)	$4L/\delta^2 \cong \infty$	app. 44	app. 15.4
Density (A/V)	1	1/R	1

A combination of density and shape characterization appears to

give a clearer seperation than the single parameters do. Consequently, the measurement of P, A and R simultaneously and conversion to shape and density parameters seem necessary to uniquely chracterize the myctophids. For example, hatchet fish would characterize closer to a circle than myctophids while the stomiatoids would chracterize closer to a line. Although length is a parameter, by itself is not enough of a discriminant. Shape and density characterization are necessary to recognize. Of course, to determine the uniqueness of this type of chracterization, this type of analysis must be performed for every family of nekton expected. However, it appears that geometric characterization by itself is not enough of a discriminant for a practical recognition system. Geometric characterization combined with perhaps bioluminescence,which is described below, might provide the unique signature for a computer recognition system.

C. Characterization of Bioluminescence

Characterization by bioluminescence is being considered as it presents the possibility of recognizing "species" of myctophids. This stems from the fact that each species has developed its own spatial arrangement of photophores. An optical/computer system programmed to recognize according to the spatial arrangement of the photophores could in principle count species of myctophids. This is strengthened by the belief that myctophids have the ability to recognize members of their own species from the photophoric arrangement. In figure 12 is depicted the spatial arrangement of the photophores of 5 species from the myctophid genus Diaphus. As illustrated, even though the photophoric arrangement is similar, they are not exactly the same.

In addition to the photophoric arrangement, a second discriminant is available for use in recognition consisting of the frequency of bioluminescent flashing. Although less is known about this aspect of bioluminescence, it should provide a discriminant against sunlight scattered background when designing a system. Further inputs are required from the marine biological community in order to assess this parameter as a means of recognition.

In order to design a system that can use bioluminescence as a parameter in its recognition system, an estimate is necessary of the intensity level of bioluminescence that can be expected from individual lantern fish.

Two approaches are utilized in trying to arrive at an estimate of the individual's bioluminescent intensity.

1) Estimate Based on Scattered Background

Bioluminescence in the twilight zone may take the place of countershading in surface waters. If the intensity of a fish's belly lights matches the intensity of sunlight filtered into the twilight zone, the fish will create silhouette nor shadow when seen from below. If lantern fish use this mechanism to reduce their visibility to predators, then an estimate can be made of the intensity of bioluminscene by equating it to the filtered sunlight background in the twilight zone.

The depth of the twilight zone is determined by the surface illumination of the sun or moon. Echograms taken off of San Diego[5] indicate the following scenario. An hour before sunrise, the various organism of the deep scattering layer (DSL) begin their descent. The myctophid, the most sensitive to light, generally start down first because they must dive to the darkest depths. A short time later the

second layer, believed to be the euphasiids, takes form and settles and soon to be followed by a third layer believed to be composed of sergestid shrimps. The layers never cross, indicating that each family of the DSL seeks its own level of illumination. Diving at speeds of 25 feet per minute, the scatterers are at least halfway to their ultimate levels at sunrise. Within an hour after sunrise they attain their preferred depth. As the sun approaches zenith, they sink a bit lower to their maximum depth.

The level sought by each organism apparently seems to depend on the organism's sensitivity to light. In a bathyscaph dive off of San Diego[5], there were no large organisms found between 850 to 1200 feet. Between 1200 to 1500 feet deep-sea prawns were seen, so many in fact, that they could not be counted. In the next 200 feet a large number of lantern fish were encountered. From 1700 feet to 2150 feet, there were relatively few large organisms; however, from 2150 to 2300 feet a large concentration of what were apparently lantern fish were observed. In another dive, there was an abrupt change in water clarity at 2100 feet described as crystal clear.

In addition, it has been observed[5] that bright moonlight holds the DSL at shallow depths although what is meant by shallow depths is not quantified in the reference.

In order to arrive at some estimate of bioluminescence, we could take the level of illumination at each depth and equate it to the exponential decay of light through clear ocean water. However, level of illumination is characterized in terms of human cone vision (light adapted eye) while the fish response is in term of their own vision different from man's. Consequently, in order to relate the above

scenario to the subjective response of fish vision, we must recast the known levels of illumination at various times of the day or night into illumination values as the fish "sees it".

The problem can be simplified if we assume that the source of illumination (e.g. sunlight, moonlight and starlight) can be characterized as a white light source (i.e. uniform intensity per unit wavelength). For noonday sunlight this is approximately true while starlight and moonlight, at least over the wavelengths of interest, can also be characterized as "white".

The defining equation for subjective response given the radiance of a source in objective (e.g. watts/cm^2·micron) can be written as,

$$\mathcal{L} = V E_\lambda \int_{\lambda_1}^{\lambda_2} K_\lambda \, d\lambda \qquad (62)$$

where $\mathcal{L}$ = subjective response (lumens/cm^2)

V = conversion factor (lumens/watt)

E_λ = radiance of source (watts/cm^2 micron)

K_λ = Visibility curve (normalized to 1.00 at peak sensitivity)

For man, two kinds of response are recognized; the cone vision (light adapted eye) and rod vision (dark adapted eye). For most fish there is only one kind of vision, namely, rod vision. For man we have the following values for V[7].

V(cone) = 680 lumens/watt @ 555 nanometers

V(rod) = 1724 lumens/watt @ 513 nanometers

In order to obtain a value of V for fish, we note that it has been determined that the density of retinal rhodopsin for man is about

.15 while for midwater fish it is greater than 1.0. Although estimates of light absorbed/cm^2 of retina/sec has been put at 15 to 30 times greater for fish than humans, we take a conservative estimate of 12 times for this evaluation and take V(fish) at about 20,000 lumens/watt at 480 nanometers.

The next step in this conversion process is the evalution of in equation (62). For man's cone vision it is .1068 microns and for man's rod vision it is .0891 microns[7]. We assume that the general shape of the fish visibility curve is similar to man's rod vision with a peak at 480 nanometers instead of 513 nanometers and extends from 480 to 550 nanometers instead of 400 to 650 nanometers. The two curves used for this evaluation is shown in figure 13. If we take the limit of man's cone vision as 400 to 700 nanometers, we note that the equivalent width of the visibility curve is .1060 microns/.3 microns or 35.6% of the limits of vision. Similarly, for man's rod vision it is about .0891/.25 or 35.6% of the limits of vision. If the visibility curve of fish vision is similar to man's we have that the equivalent width is .356(.15) or about .053 microns.

We are now in a position to estimate $\mathcal{L}$ for fish according to equation (62). Based on the response of midwater fish, they are found grazing at the surface of the water when there is no moonlight. For a clear starlight night, the level of illumination on a horizontal surface is about 3×10^{-8} phot[8] (lumens/cm^2)- rod vision (man), (rod vission occurs when the eye becomes adapted to a field luminance below 10^{-2} candles/m^2 for at least 30 minutes[9]. From equation (62) we have that,

$$E_\lambda(\text{night}) = \frac{3 \times 10^{-8}}{1724\,(.0891)} \cong 2 \times 10^{-10} \text{ WATTS/CM}^2\cdot\mu \qquad (63)$$

For fish vision this level of irradiance produces,

$$\mathcal{L}(fish) = 2 \times 10^{4}(2 \times 10^{-10})(.053) \cong 2 \times 10^{-7} \text{ Lumens/cm}^2 \quad (64)$$

We could call this fish-lumens or ichthylumens to indicate fish response but will retain the term lumens and just indicate when it refers to the fish vision response. It is noted that compared to man's rod vision, the fish vision response is only approximately 7 times greater than man's due to the narrower vision bandpass. As we will discover below, this changes dramatically in deep water.

In deep water, due to the spectral attenuation of sea water, in order to use equation (62), we would have to move the E_λ under the integral. To avoid this complication, we note that in deep water, the resultant radiance becomes very monochromatic with a peak at about 480 nanometers. Based on the measurements made by the DOOM project[10] a change of only 10% in α with wavelength will produce a monochromatic radiance confined to 480 ± 10 nanometers. Consequently we can treat the E_λ as still constant over this bandpass.

Referring to figure 13 we have graphically intergrated a 20 nanometer bandpass over both the fish visibility and man's rod visibility curves with the result that for fish vision the equivalent width is about .02 μ while for man's rod vision it is about .013 μ. As fish are at their greatest depths for a zenith sun, the E_λ to use in equation (62) is the radiance due to noonday sunlight. Terrestrial sunlight has a radiance value on a horizontal surface of about .15 watts/cm^2 micron [11]. Consequently,

$$\mathcal{L}(fish) = .15(2 \times 10^{4})(.02)e^{-\alpha_0 R} \quad (65)$$

where α_o = attenuation coefficient for sea-water at 480 nanometers

R = depth

or,

$$\mathcal{L}(\text{fish}) = 60 e^{-\alpha_o R} \text{ (Lumens/cm}^2\text{)} \tag{66}$$

Similarly for man's rod vision,

$$\mathcal{L}(\text{man}) = 3.36 e^{-\alpha_o R} \text{ (Lumens/cm}^2\text{)} \tag{67}$$

As can be seen, fish vision is now about 18 times as sensitive as man's vision for filtered sunlight.

We now equate equation (64) to equation (66) as it is known empirically that fish can tolerate this level of illumination. Hence,

$$2 \times 10^{-7} = 60 e^{-\alpha_o R} \tag{68}$$

or,

$$\alpha_o R_{max} = 19.52 \tag{69}$$

This indicates that the maximum will be determined by α_o, the average attenuation coefficient at 480 nanometer. For typical ocean water, neglecting the surface attenuation, $\alpha_o \cong .05$ meter^{-1}. From equation (69) Rmax becomes about 390 meters. For clearest ocean water $\alpha_o \cong .033$ with R_{max} = 590 meters. Consequently, midwater fish, based on this analysis, should be found between 1300 to 2000 feet during the daytime. This correlates well with the observations made

from the bathyscaph. This analysis also explains why moonlight will drive the fish into shallow depths. An estimate of the depths reached can be made by taking the equivalent width as .04 microns instead of .02 microns. A full moon produces an illumination of about 1.6×10^{-5} phot (cone vision). Hence,

$$E_\lambda(\text{moonlight}) = \frac{1.6 \times 10^{-5}}{680(.1068)} = 2.2 \times 10^{-7} \frac{\text{WATTS}}{\text{CM}^2 \cdot \mu} \tag{70}$$

and,

$$\mathcal{L}(\text{fish-moonlight}) = 2.2 \times 10^{-7}(2 \times 10^4)(.04)e^{-\alpha_0 R} \tag{71}$$

or,

$$\mathcal{L}(\text{fish-moonlight}) \cong 1.8 \times 10^{-4} e^{-\alpha_0 R} \tag{72}$$

Again equating to equation (64) we have,

$$2 \times 10^{-7} = 1.8 \times 10^{-4} e^{-\alpha_0 R} \tag{73}$$

or,

$$\alpha_0 R = 6.80 \tag{74}$$

Typically for surface waters, $\alpha_0 \cong 0.15$ and R becomes 45 meters. For $\alpha_0 \cong .10$, R= 68 meters. Consequently, moonlight can drive the fish a couple hundred feet below the water's surface.

In order to complete the scenario, we now estimate the range of illumination that the midwater fish can tolerate. It was stated above that lantern fish do not begin their descent until an hour before sunrise. The level of illumination 1 hour before sunrise is dependent on latitude and time of year. For example, for middle latitudes and June 21, the solar depression angle is about 7^{o}[12]. For this depression angle, the illuminance on a horizontal surface is about 10^{-4} phot (cone vision)[13]. Again from equation (64),

$$E_{\lambda} = \frac{10^{-4}}{680(.1068)} \cong 1.4 \times 10^{-6} \frac{\text{WATTS}}{\text{CM}^2 \cdot \mu} \qquad (75)$$

For fish vision this becomes for shallow water,

$$\mathcal{L}(\text{fish}) = 1.4 \times 10^{-6}(2 \times 10^{4})(.04)\, e^{-\alpha_o R}$$

$$\cong 1.1 \times 10^{-3} e^{-\alpha_o R} (\text{Lumens}/\text{CM}^2) \qquad (76)$$

Since the exact lighting conditions are not given in reference[5], we must assume that 1 hour before sunrise is near moonset and the lantern fish were in shallow water before they started their descent. Using the value of $\alpha_o R$ in equation (74) we have that,

$$\mathcal{L}(\text{fish}) = 1.1 \times 10^{-3} e^{-6.80} (\text{Lumens}/\text{CM}^2) \qquad (77)$$

or,

$$\mathcal{L}(\text{fish}) \cong 1.2 \times 10^{-6} (\text{Lumens}/\text{CM}^2) \qquad (78)$$

This result is independent of depth and only presumes that the equivalent width for the fish eye visibility is about .04 μ . This indicates that the lantern fish can tolerate at least 10 times the normal lighting conditions, presumably due to the time required for their eyes to accomodate to changing light conditions similar to man's vision.

If the above analysis correctly accounts for the observed scenario of lantern fish, then we can conclude that the level of illumination at equilibrium equals at least the level of their bioluminescence. Therefore at great depths we have that,

$$I = .15\,(.02)\,e^{-\alpha_o R} \ (\text{WATTS/CM}^2) \qquad (79)$$

Since $\alpha_o R = 19.52$ from equation (69), we have that the intensity of their bioluminscence per animal is about 10^{-11} watts/cm^2 or $10^{-5}\mu$ watts/cm^2 at 480 nanometers with a bandpass of $\pm$ .01 μ.

The results of this anlysis are collected and shown in Table 1 for convenience.

2 Measured Bioluminescence

During the diurnal migration of the scattering layer in deep water adjacent to the Canary Island, the layer was shown to closely follow the isolume of $5\times10^{-4}\mu$ W/cm^2 at 474 nanometers. In addition, the layer did not begin their descent until about 1 hour before sunrise where they were in shallow waters at about 100 meters due to moonlight. Although this was not measured from a single animal but a school, the measurements correlates well with our estimate of $10^{5}\mu$-watts/cm^2 per animal.

In addition, Nicol[14] has measured the luminescence of a number of animals and, for long lasting flashes, he gives values ranging from 10^{-9} to 2×10^{-5} μ W/cm^2 on a receptor surface placed 1m from the source and normal to it. For a single animal approximately 1x5cm, and assuming diffuse radiation, the radiance is about $\frac{5}{\pi} \times 10^{5}$ μ W/steradian using our estimated value of luminescence . A receptor 1 meter away, assuming a point source of radiation, would produce an irradiance of $\frac{5}{\pi} \times 10^{-9}$ μ W/cm^2. This is close to the lower limit given by Nicol. As it is not indicated whether the radiance measured was from a single animal or a group, we conclude that our estimate is a reasonable one. Consequently, in future analyses , we will retain the value of 10^{-5} μ W/cm^2 per animal when estimating sensitivity requirements for detection.

TABLE I

COMPARISON OF MAN'S VISION WITH FISH VISION TO EST
LEVEL OF FISH BIOLUMINESCENCE (SEE TEXT)

	V (Lumens/Watt)	$\int K_\lambda d\lambda$ (Microns) to white light	λ (Nanometers) wavelength of maximum sensitivity	$\mathcal{L}$ (1) (Phot) Starlight at surface of water	$\mathcal{L}$ (Phot) Zenith sun in deep water	$\int K_\lambda d\lambda$ (Microns) In deep water
MAN (Cone Vision)	680	.1068	555	---	---	---
MAN (Rod Vision)	1724	.0891	513	3×10^{-8}	$3.36e^{-\alpha_o R}$	.013
FISH (Rod Vision)	20,000*	.053	480	2×10^{-7}	$60e^{-\alpha_o R}$	.020

*Estimated (See Text)

1. $\mathcal{L} = V E_\lambda \int_{\lambda_1}^{\lambda_2} K_\lambda d\lambda$ $\mathcal{L}$ in phots (Lumen/cm^2)

(See Text For Definitions of Other Symbols)

SION TO ESTIMATE THE
TEXT)

$\int K_\lambda d\lambda$ (Microns) In deep water	$\int K_\lambda d\lambda$ (Microns) In shallow water	$\mathcal{L}$ (Phot) Shallow Water Moonlight	$\mathcal{L}$ (Phot) Tolerable Level One Hour Before Sunrise	$\alpha_o R$ Deep Water	$\alpha_o R$ Shallow Water	I (Watts/cm^2) Bioluminescence per Animal
---	---	---	---	---	---	---
.013	---	---	---	---	---	---
.020	.04*	$1.8 \times 10^{-4} e^{-\alpha_1 R}$	1.2×10^{-6}	19.52	6.80	10^{-11}

12

V. OPTICAL PATTERN RECOGNITION

A. Background:

Although the orginal intent of this program was to develop a recognition system utilizing a computer recognition scheme, it has become apparent during the course of this work that such a system will not meet the design criteria of a viable recognition and counting system. This change in direction is the result of the following requisite characteristics of a recognition and counting system:

(a) due to the increased costs of available ship time, a towed fish must move more rapidly to gather more data in a shorter time than originally envisioned (i.e. from 1 knot to 10 knots).

(b) due to the enormous costs involved in testing any counting system in the ocean, it is more desirable (i.e. economically and for purposes of calibration) to be able to test a developed system on a simulator that can reasonably imitate the following variables encountered in ocean testing:

1) motion of the towed fish
2) sea transfer function with range
3) orientation of nekton
4) background scattering
5) attenuation of the sea water
6) detector characteristics
7) bioluminescent characteristics of the nekton

The inability of present day computer technology to cope with requirement (a) above can be seen from the following considerations. Assuming a modest image format of 100x100 image elements (i.e.regardles of how the image is formed), a relative motion between the towed fish and nekton of 10 knots (about 500 cm./sec.) will produce

a smearing of each object point or resolution element. A modest resolution element in object space for lantern fish is about 1mm. To minimize object blur and hence image blur, we require the blur to be no more than 1/10 of the resolution element or .1 mm to maintain the image quality of the static case. Taking a worst case situation, we require that each resolution element be recorded in $2x10^{-5}$sec. For a 100x100 image format, this results in an image being recorded every $2x10^{-5}$ sec. In a sequentially recorded system, this results in a pixel (i.e. picture element) transmission rate of $5x10^{8}$/sec. If 4 bits represents each pixel (16 levels of grey), then we need a transmission rate of $2x10^{9}$ bits/sec. This is well beyond the state-of-the art for small systems. Although this is a worst case situation and under certain situations the rate is well below this, if the system is to be usable in the real world, we conclude that sequential processing cannot be used. Parallel processing becomes necessary in order to achieve the required image quality under high towing rates. This suggests that optical processing should be used if possible. Although optical processing is not at the stage of development that image computer processing is, it is sufficient to meet the requisite constraints for a viable counting system.

The second constraint, (b) above, suggests the use of optical processing also for the simulator. As will be shown below, proper optical design will reasonably simulate the listed variables above using incoherent light.

B. Theory:

1. Background:

It would take us too far afield to describe fully the theory of of image formation using the concept of linear spatial filter theory. Many excellent texts have been written describing the theory. The

text by O'Neill[15] is the classic in the field. We only present here the salient features of the theory in order to describe both the simulator and the optical image processing proposed for this work.

In incoherent light, an image formed by any optical system can be considered to be the convolution of the system spread function s(x) (i.e. response of the optical system to a point source) with the object intensity distribution $O(\epsilon)$. Here x and ϵ refer to two dimensions. Hence we can write,

$$I(x) = s(x) \odot O(\epsilon) \tag{80}$$

where, I(x) = resultant image intensity distribution

$\odot$ = mathematical convolution

Fourier transforming (1) results in,

$$I(\omega) = \tau(\omega) \cdot O(\omega) \tag{81}$$

where, $I(\omega)$ = image optical spatial frequency spectrum

$\tau(\omega)$ = optical tansfer function

$O(\omega)$ = object spectrum

ω = optical spatial frequency

It is noted that whereas there is a convolution in image space, there is simple multiplication in frequency space.

Since s(x) can be written as,

$$s(x) = A(x) \cdot A^*(x) \tag{82}$$

where, A(x) = amplitude image distribution function

$A^*(x)$ = complex conjugate of A(x)

Then, the Fourier transform of s(x) becomes,

$$\tau(\omega) = P(\omega) \odot P^*(\omega) \qquad (83)$$

where, $P(\omega)$ = exit pupil function expressed in spatial frequency units

$P^*(\omega)$ = complex conjugate of $P(\omega)$

Consequently, the effect on imaging by an optical system can be modified according to the form of the exit pupil of the system. The resultant modification on $\tau(\omega)$ produces the kind of image quality formed in frequency space. The mathematical operation of convolution (autocorrelation for a symmetric function) for a symmetric pupil function is simply the translation of the pupil function over itself. In many cases, this can be done graphically. For example, for a rectangular pupil function, the resultant $\tau(\omega)$ is a linear decreasing function. For other pupil functions, more complicated $\tau(\omega)$'s result.

2. Optical Simulation Of Sea Parameters:

From an economical point of view and in terms of calibrating and determining the effectiveness of a developed recognition and counting system, it is desirable to be able to simulate those parameters that will be encountered in sea testing. Although, all the parameters cannot be simulated exactly, enough of the important parameters can be simulated so that the performance of a developed system can be experimentally verified without sea testing.

(a) Simulation of Uniform Motion in One Direction:

It can be shown[2] that linear motion of the image in one direction will affect the transfer function according to,

$$\tau(\omega_x) = \tau_o(\omega) \sin(\omega_x L/2)/\omega_x L/2 \qquad (84)$$

where, $\tau_o(\omega)$ = transfer function for static image

L = v times t

v = velocity of moving image

t = integration time

From equation (83) the transfer function can be represented by the autocorrelation function of the pupil function. Consequently we need a representation for,

$$P(\beta)\, P^*(\beta-\omega_x) \tag{85}$$

For pure phase variations, that is for $P(\beta) = e^{-i k \Delta(\beta)}$, a phase error of the form $\Delta(\beta) = a_n \beta^n$ produces an integrand in equation (83) of the form,

$$P(\beta)\, P^*(\beta-\omega_x) = e^{+i k w(\beta, \omega x)} \tag{86}$$

where, $w = \Delta(\beta) - \Delta(\beta-\omega_x)$ is a polynomial of degree n-1 in β. For n = 2, the resultant polynomial represents a focussing error of the form $\Delta(\beta) = b_1(\beta/\beta_0)^2$ where,

$$\beta_0 = \frac{2\pi a}{\lambda F} \tag{87}$$

with a the radius of the pupil, F, the focal length of the lens and b_1, the magnitude of the focussing error given by,

$$b_1 = \frac{a^2 \Delta l}{2F^2} \tag{88}$$

with Δl = the distance the lens is out of focus. It can be shown [16] that when b_1 is greater than 2λ, the resultant transfer function is,

$$\tau(\omega_x) = \frac{\sin(\omega_x d)}{\omega_x d} \tag{89}$$

where 2d is the diameter of the defocussed spot (geometrical approximation).

For b_1 greater than 2λ we have that,

$$\frac{a^2 \Delta l}{2F^2} \geq 2\lambda \tag{90}$$

or,

$$\Delta l \geq 16 \lambda F_{\#}^2 \tag{91}$$

where $F_{\#}$ = f number of the lens. From equation (84), we find the equivalence as,

$$L = 2d \tag{92}$$

or L represents the diameter of the defocussed spot size. Consequently, defocussing in one demension is optically equivalent to linear image motion and the magnitude of L can be simulated by the amount of defocussing through equation (91) . Finally image motion can be related to object motion by knowing the object range.

(b) Sea Transfer Function With Range:

It has been shown by Wells [2], that the transfer function for sea image transmission can be written as,

$$\tau(R, \Psi) = e^{-D(\Psi)R} \tag{93}$$

where $D(\Psi)$ = decay function/distance

R = range

Ψ = spatial frequency in terms of radians (frequency) per radians (angle).

It has been shown by Wells that for the focussed case,

$$D(\psi) = \alpha - \frac{s\left[1 - e^{-\psi\theta_0}\right]}{\psi\theta_0} \tag{94}$$

where α = attenuation coefficient

s = scattering coefficient

θ_0 = characteristic angle of the volume scattering function

Consequently, the sea scattering parameters and attenuation can be used to determine the $\tau(R,\psi)$ directly. Calling $[1-e^{-\psi\theta_0}]/\psi\theta_0$, γ, equation (94) becomes $D(\psi) = \alpha - s\gamma$ or,

$$\tau(R,\psi) = e^{-\alpha R} \cdot e^{s\gamma R} \tag{95}$$

where $0 \leq \gamma \leq 1$. When $\gamma = 0$, $\tau(R,\psi) = e^{-\alpha R}$ and there is no scattering. When $\gamma = 1$, $\tau(R,\psi) = e^{-(\alpha - s)R}$ or $e^{-\gamma R}$ where γ is the broad bean attenuation coefficient. Consequently, $\tau(R,\psi)$ at $\psi = 0$ is $e^{-\gamma R}$ and decays exponentially to $e^{-\alpha R}$ as $\psi \to \infty$.

In order to simulate this function in τ, we need an attenuation given by $e^{-\gamma R}$ with an exponentially decaying function according to equation (95). An excellent approximation to this function can be obtained optically by considering the spherical aberration of a lens. From equation (86) and what follows there, when $n = 4$ we have that,

$$\Delta = C_1 \left(\beta/\beta_0\right)^4 \tag{96}$$

which represents spherical aberration at the paraxial focus. The magnitude of C_1 is given by,

$$C_1 = \frac{\Delta L}{F_\#^2} \tag{97}$$

where ΔL = distance between the paraxial focus and marginal focus. By irising the lens, the value of ΔL can be varied to simulate different amounts of spherical aberration and hence varying degrees of exponential decay. By suitably choosing the $F_{\#}$ and the shape factor of the lens, a wide range of the sea transfer functions can be simulated in a continous fashion.

(c) Orientation, Background Scattering And Attenuation:

Orientation is simply accomplished by object rotation, while background scattering is introduced seperately as background light and attenuation is simulated by crossed polarizers in the system.

(d) Detector Characteristies:

In the above analysis it was tacitly assumed that the image resolution was controlled by the transfer function. Under conditions of weak illumination, the system becomes noise limited rather than transfer limited. The relating equations in terms of threshold contrast requirements have been developed by Hodara [17] and are based on the premise that the threshold detector contrast is given by,

$$C_D = SNR/\sqrt{N_t} \tag{98}$$

where C_D = threshold detector contrast

N_t = total number of photons per unit area

He has shown that equation (98) can be cast into terms of the detector characteristics as,

$$SNR \cdot \nu = C_D \sqrt{\frac{Q N_t}{1 + N_n/N_t}} \cdot \tau(\nu) \tag{99}$$

where, ν = spatial frequency (cycles/mm)

Q = quantum efficiency of the detector

N_t = total number of photons /mm^2

N_n = noise photons /mm^2

$\tau(\nu)$ = transfer function

For weak illumination and low resolution $\tau(\nu)=1$ and equation (99) becomes,

$$SNR \cdot \nu = C_D \sqrt{\frac{Q N_t}{1 + N_n/N_t}} \tag{100}$$

For strong illumination and high resolution, equation (99) becomes,

$$\nu = \sqrt{Q N_t [C_D/SNR]^2}\, \tau(\nu) \tag{101}$$

or transfer limited. For each detector type, specified by Q and N_n, a plot of $SNR \cdot \nu / C_D$ versus N_t for weak illumination determines the detector requirements. For the strong illumination case, a plot of ν versus $N_t (C_D/SNR)^2$ determines the detector's "seeing" ability. In either case, the dominance of either N_n or $\tau(\nu)$ will be determined by detector type and N_t. To simulate the different conditions, it is only necessary to monitor N_t in the image and the detector seeing ability can be determined from equation (99) with input parameters of SNR, C_D, Q and N_n. It is proposed to simulate this parameter by simply measuring the photon flux in the image plane and relating this to the detector characteristics through equation (99).

e)Bioluminescence Simulation:

We have shown in section IV-C,using as an illustration the myctophid genus Diaphus, that the spatial arrangement of the photophores in principle might be used for identification of the myctophid species.

Due to the expected high data rate necessary, it appears that this would be extremely difficult. However in order to experimentally verify this, it is proposed to simulate the biolumescent photophores as follows.

In the input object plane, a mask is prepared simulating the photophoric arrangement. This is diffusely illuminated in monochromatic light of controlled intensity ($\lambda \sim 480$ nm) and passed through the simulator. The various parameters are applied and the resultant image is examined either visually or eventually with the pattern recognition system. The results of this type of testing will determine whether this parameter is a viable means of identifiction.

f) Summary :

The seawater optical simulator to produce the various effects discussed above is shown in figure 14. The input object to be used can be film or direct projection from a specimen of lantern fish. If film is used as the input, 35mm transparencies can be prepared from photographs taken of the specimens of lantern fish found for example at the Smithsonian Institute.

3. Optical Pattern Recognition:

As mentioned above, due to the rapid towing rates desired for the recognition and counting system, it appeared that computer sequential image processing is not adequate and a parallel processing system is necessary.

It is the purpose of this phase of the work to examine the practicality of using Fourier transform principles to do the recognition and counting utilizing a hybrid optical/computer system. It is intended to work entirely in frequency space as motion of the object does not affect the transform. The transform is affected by orientation, size

shape and number.

The principle to be used in developing a system is the following. In any imaging system, (disregarding the degradation due to the optics for the moment) using incoherent light, the object spectrum is the autocorrelation of the amplitude transform, i.e.,

$$\underset{\text{(Object)}}{A(\varepsilon)} \xrightarrow[\text{Transform}]{\text{Fourier}} G(\omega) \tag{102}$$

and,

$$O(\omega) = G(\omega) \odot G^{*}(\omega) \tag{103}$$

Due to the two demensional nature of the object spectrum, any asymmetry in the object will produce an asymmetrical spectrum. As the object rotates, the spectrum also rotates (orientation effect). In addition, the size of the object will determine the magnitude of the high frequency components while the shape determines the asymmetry in the spectrum. Also if two similar objects are in the field of view of the optical system in the same orientation, the resultant spectrum is the same but with twice the intensity. If three, then three times the intensity and so on.

In principle, if the resultant spectrum can be harmonically analyzed radially, the average size and shape can be determined and from the strength, the number of objects. In dealing with schools of lantern fish,(i.e. numbering in the thousands) it is not expected to be able to count the number exactly but to acheive average number, average size etc. as the fabrication of a system to count individually would be an enormous task.

In an incoherent system, it is not possible to work directly in frequency space (i.e. a physical plane) but by the judicious use of

masks and lens aberrations, the object spectrum can be analyzed due to the relationship,

$$I(\omega) = \tau(\omega)\, O(\omega) \tag{104}$$

where the $\tau(\omega)$ of the optical system can be varied to analyze the $O(\omega)$. For example, if two slits are place in the exit pupil of the system, the $\tau(\omega)$ consists of a d-c term plus spectral components at $\omega_o = \pm 2\beta_o$. By varying the distance of the slits, we are in effect harmonically analyzing the structure of the object intensity distribution. An annulus in the exit pupil effectively does the same thing except radially.

It will be the purpose of this part of the work to develop ways of:

1) radially varying the $\tau(\omega)$
2) asymmetrically varying the $\tau(\omega)$
3) determining the effects on the object spectrum

In order to keep pace with the rapidly varying object distribution, the variations in $\tau(\omega)$ must be made rapidly- possibly mechanically or even electro-optically.

To expand on the principle to be used in optical pattern recognition and counting, we utilize the geometry depicted in figure 15. Here, $O(\xi)$ represents the object (objects) intensity distribution, $P(\omega)$ represents the pupil amplitude distribution at the exit pupil of the optical system (expressed as frequency units),and I(x) the image plane intensity distribution where the measurements are made. Depending on the number of objects in the field of view at a given time, we denote the $O(\xi)$ as,

$$O(\varepsilon) = \alpha_1 f_1(\varepsilon) + \alpha_2 f_2(\varepsilon - b_1) + \alpha_3 f_3(\varepsilon - b_2) + \cdots \qquad (105)$$

where the α's reflect the maximum radiance from the objects (i.e. product of illuminating source density and diffuse reflectivity of the objects), the f's represent the radiance distribution of each object and the b's represent the location of each object referred to the center of the optical system. Equation (105)is Fourier transformed in intensity and utilizing the linearity and shift theorems, and can be written as,

$$O(\omega) = \alpha_1 g_1(\omega) + \alpha_2 g_2(\omega) e^{i\omega b_1} + \alpha_3 g_3(\omega) e^{i\omega b_2} + \cdots \qquad (106)$$

In the case of a school of fish of the same family (i.e. approximately the same size with equal relectivities and oriented in the same direction), we can write,

$$O(\omega) = N \alpha g(\omega) \left[1 + e^{i\omega b_1} + e^{i\omega b_2} + \cdots\right] \qquad (107)$$

where N = the number of objects.

If the distribution of the fish is random but the same orientation, then the linear phase shift terms do not acquire a finite mean value and except for local fluctuations equation (107)becomes,

$$O(\omega) = N \alpha g(\omega) \left[1 + \text{residual}\right] \qquad (108)$$

From equation (83) we stated that the incoherent transfer function of the optical system can be expressed as,

$$\tau(\omega) = P(\omega) \odot P^*(\omega) \qquad (109)$$

where $P(\omega)$ is the pupil function. Combining this with equation(108), we have that,

$$I(\omega) = O(\omega) \cdot \tau(\omega)$$
$$I(\omega) = N\alpha\, g(\omega) \cdot P(\omega) \odot P^*(\omega) \qquad (110)$$

Transforming (110) results in,

$$I(x) = N\alpha\, f(\varepsilon) \odot \widetilde{P(\omega)} \cdot \widetilde{P^*(\omega)} \qquad (111)$$

where $\widetilde{P(\omega)}$ is the transform of the pupil function. Hence,

$$I(x) = N\alpha f(\varepsilon) \odot \left|\widetilde{P(\omega)}\right|^2 \qquad (112)$$

Effectively, equation (112) indicates that the resultant image distribution can be encoded according to the pupil function transform $\widetilde{P(\omega)}$. As the form of $P(\omega)$ is at the discretion of the system designer, it can be seen that if $P(\omega)$ is a time varying function properly chosen, the resultant intensity distribution variation can be used to determine N if α and $f(\varepsilon)$ are known (i.e. shape size and reflectivity). In addition, due to the asymmetry of the nekton, the time variation of $P(\omega)$ must be done in such a way that the asymmetry can be measured. This will be the main thrust of this phase of the work.

As an example of how $P(\omega)$ affects the image coding, a simple form for $P(\omega)$ is an annulus described mathematically as a radial delta function,

$$P(\omega) = \delta(\omega - \omega_o) \qquad (113)$$

where ω_o is the location of the annulus. It can be shown that the Fourier-Bessel transform of (113) is,

$$\widetilde{P(\omega)} = \omega_o J_o(\omega_o x) \qquad (114)$$

Consequently,

$$|P(\omega)|^2 = \omega_o^2 |J_o(\omega_o x)|^2 \tag{115}$$

Substituting into equation(112) we have that,

$$I(x) = N\alpha\omega_o^2 \int f(\varepsilon) |J_o[\omega_o(x-\varepsilon)]|^2 d\varepsilon \tag{116}$$

Now, if the entire image is integrated then,

$$\int I(x)\,dx = N\alpha\omega_o^2 \iint f(\varepsilon) |J_o[\omega_o(x-\varepsilon)]|^2 d\varepsilon\,dx \tag{117}$$

or,

$$N = \frac{\int I(x)\,dx}{\omega_o^2 \alpha \iint_{\text{ENCODED IMAGE}} f(\varepsilon) |J_o[\omega_o(x-\varepsilon)]|^2 d\varepsilon\,dx} \tag{118}$$

Since ω_o, α and $f(\varepsilon)$ are known, measurement of the total integrated image produced by the restricted pupil function is directly related to number.

It is to be noted that equation(118) is independent of the fish motion as long as the fish are in the field of view. This technique relaxes immeasurably the previous requirement of limiting the image analysis to 1/10 of a resolution element. Consequently, instead of requiring 50,000 frames/sec., we require that the harmonic analysis be made during the transit time in the field of view. For example, at a relative speed of 10 knots (5 meters/sec.) with a minification ratio of 100:1 and an image format of 5cm.x5cm., the pupil function is to varied once a second. This allows the use of mechanical variation instead of electro-optical which reflects the simplification

obtained by parallel processing

In the above analysis, it was assumed that the school of fish were oriented in the same way. Under real conditions, this may not be the case and only the average size and number will be obtained depending on the weighting factors of the radiance of each object. Additionally, it is to be recognized that equation (117) admits to unique solutions in N and $f(\mathcal{E})$ when ω_o is varied in a prescribed manner. In other words for a fixed N and α, only one combination of $\int I(x)dx$ with ω_o is consistent with a given $f(\mathcal{E})$.

VI. CONCLUSIONS AND RECOMMENDATIONS

The primary motivation for this study was the recognized need to augment existing methods for sampling mid-water nekton. Generally, the need for a pattern recognition system to recognize and count has become apparent during the course of this study. For high tow rates of the veiwing vehicle, the need for an optical pattern recognition technique appears to be necessary as a parallel processing computer recognition system cannot handle the high information rates that are necessary for recognition.

Specifically, we have shown in the first phase of this study that:

1) a viewing system will only be able to recognize and count nekton of grossly different morphology
2) the myctophids and euphasiids represent the lower limit of nekton recognition based on size and reflectivity
3) the viewing system must operate at relatively close range-- on the order of 20 meters-- in order to recognize the variety of nekton
4) in order to achieve the largest possible sampling volume, the illuminating beam used in the towed fish should be deployed in some circular fashion
5) resolution and hence recognition is detector limited and not limited by the sea-water transfer function
6) a viable viewing system must incorporate a recognition system to be able to count in real time the expected number and variety of nekton

In the second phase of this study, we have shown that:

7) geometric pattern recognition does appear to be a sufficient discriminant for the myctophid family of nekton

8) bioluminescence and the spatial arrangement of the photophores of the nekton might be used as a recognition parameter if a suitable recording scheme can be developed

9) under high tow rates, computer pattern recognition cannot be used and an optical pattern recognition scheme must be developed

10) the image degradation due to sea-water/detector combination can be simulated optically in the laboratory without resort to sea-trials for confirmation of the pattern recognition system

It is recommended that the next phase of this study should concentrate on developing the optical pattern recognition techniques necessary to recognize and count nekton using the myctophid family of nekton as a model. Specifically, the following items are recommended for study in future work:

1) experimentally simulate the key sea-water parameters and the detector characteristics. In particular, the following parameters should be simulated:
   a) uniform motion in one direction
   b) sea transfer function with range
   c) orientation of test objects, background scattering and sea-water attenuation
   d) detector characteristics
   e) bioluminesecence and spatial arrangement of photophores of myctophids

2) utilizing the specimen collection of myctophids at the Smithsonian Institute, prepare suitable photographic transparencies as input objects to the optical simulator

3) design of the optical pattern recognition module for myctophids

with emphasis on developing methods for rapidly modifying the pupil function of the recognition system in a prescribed manner

4) incorporate myctophid characteristics as is known by the biological community to augment the design of the myctophid recognition module

REFERENCES

(1) See reference (47), Appendix C.

(2) Willard H. Wells, Agard-LS-61, London, England (Aug. 1973).

(3) Donald E. Matlack, NOL Report 74-42 (5April 1974).

(4) Joseph W. Goodman, Introduction To Fourier Optics , McGraw-Hill Book Co., Inc.,New York (1968)

(5) Rober S. Dietz, Scientific American, 207, Aug. 1962, pg. 44.

(6) Manufacturer's Pamphelet,"G Series Solid State Scanners", Reicon Corporation, Sunnyvale, Calif., 1976.

(7) C. W. Allen, Astrophysical Quantities, University of London, The Atlone Press, London, England, 1955. pg. 103.

(8) Dr. J. A. Mauro, Optical Engineering Handbook, General Electric Co., Syracuse, New York, 1966, Section 11, pg. 39.

(9) W.E.K. Middelton, Vision Through The Atmosphere,University of Toronto Press, Canada, 1952, pg. 86.

(10) Donald E. Matlack, "Deep Ocean Optical Measurements (DOOM) Report On North Atlantic, Caribbean And Mediterranean Cruises", Naval Ordinance Lab., White Oak, Silver Spring, MD, NOLTR 74-42, April 1974.

(11) Based on a light flux of 14 phots outside of the earh's atmosphere (Reference 7, pg. 138), cone vision and a transmission for the atmosphere og 0.80.

(12) S. M. Silverman, "'It's Always Darkest Before The Dawn'???", Optical Spectra, 6, No. 4, April 1972, pg. 35.

(13) G. V. Rozenberg, Twilight, Plenum Press, New York, 1966.

(14) J. A. C. Nicol, "Observations On Luminescence In Pelagic Animals", J. Mar. Biol. Assoc. U. K., 37, 1958, pg. 705.

(15) Edward L. O'Neill, Introduction To Statistical Optics, Addison-Wesley Publishing Co., Inc., London, England, 1963.

(16) Ibid., pg. 27.

(17) Henri Hodara, Agard-LS-61, London, England (Aug. 1973).

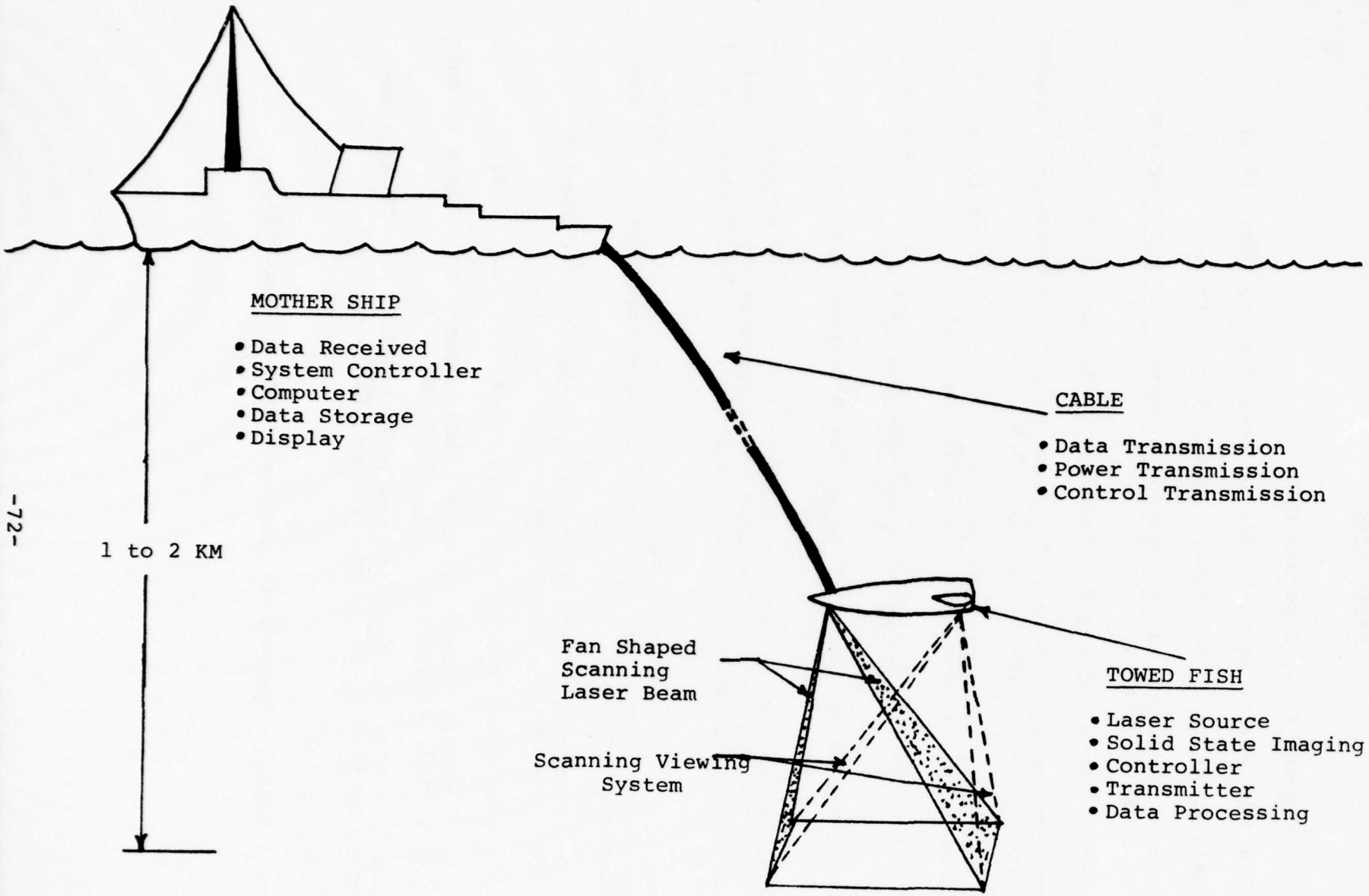

FIGURE 1. Scenario of System to View Mid-Water Nekton

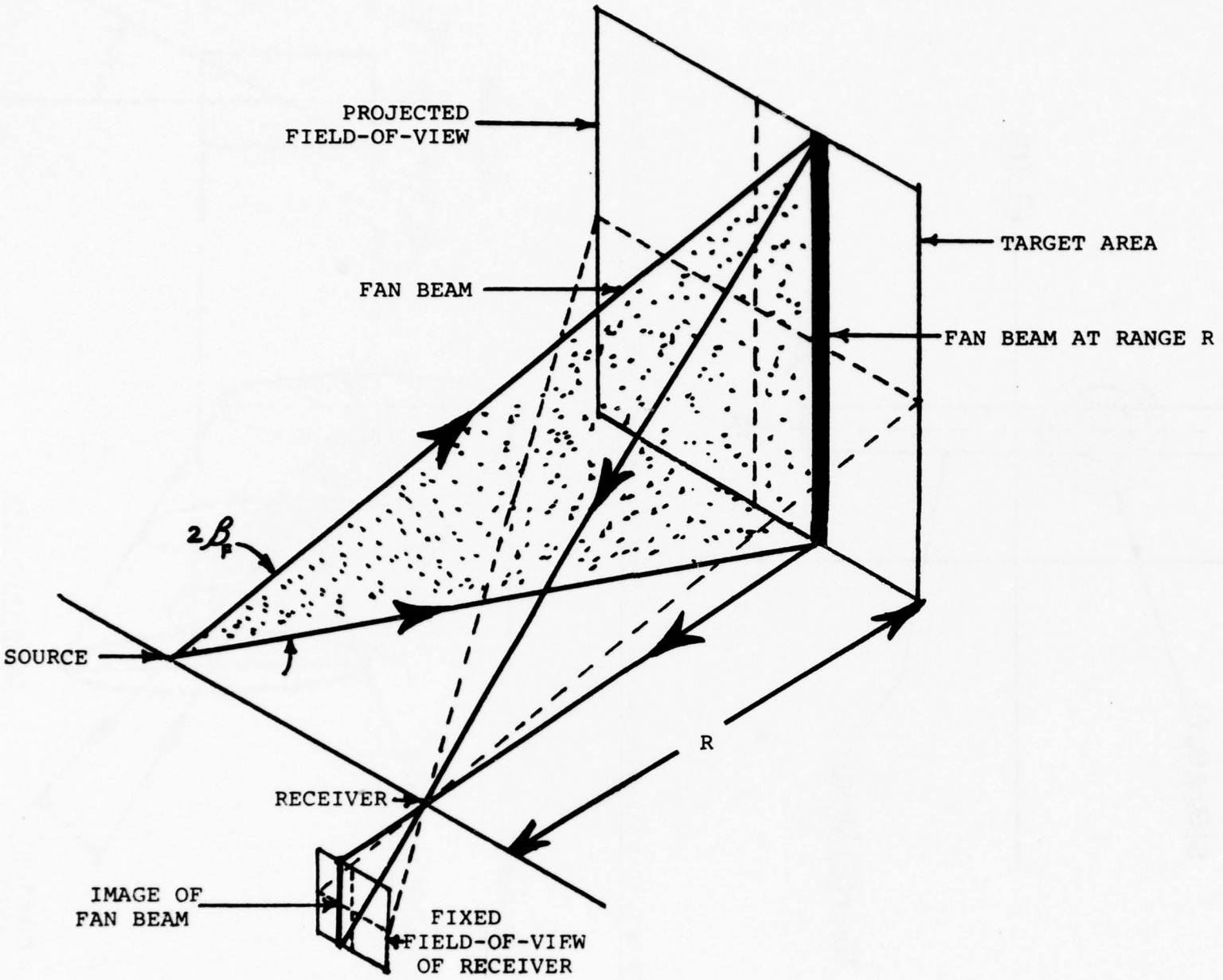

FIGURE 2. Geometry Used To Derive The Modulation Transfer Function For A Fan Beam(See Text)

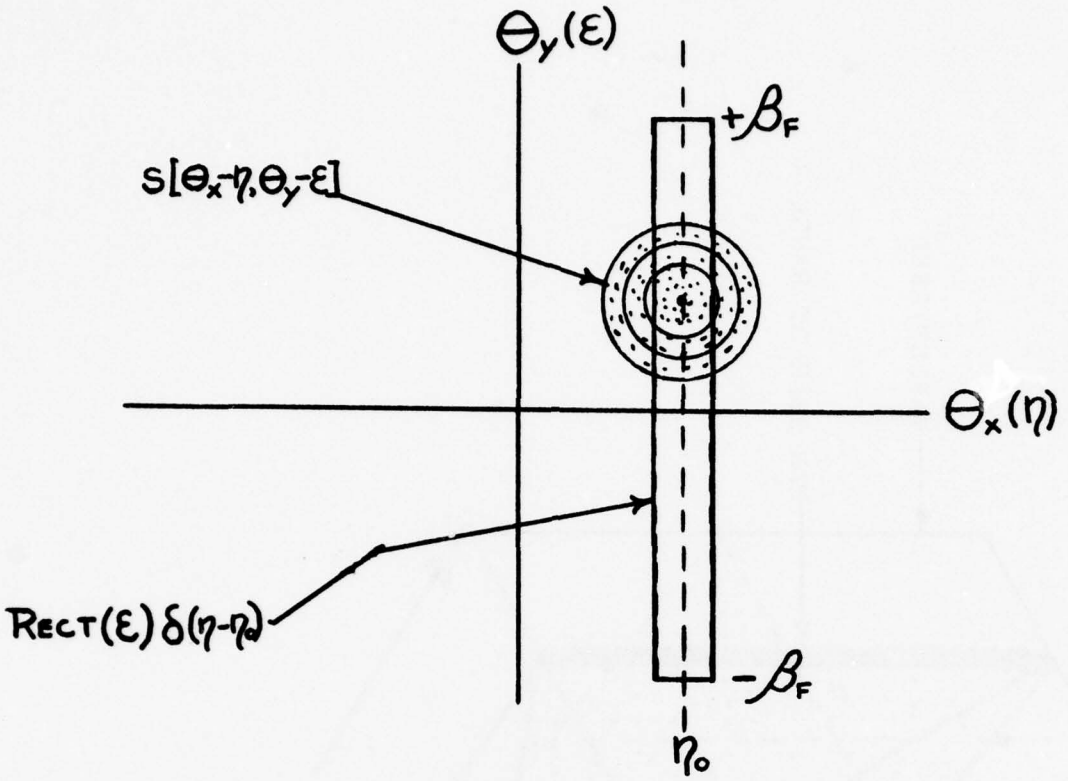

FIGURE 3. Coordinate Geometry Used To Derive The Line Spread Function

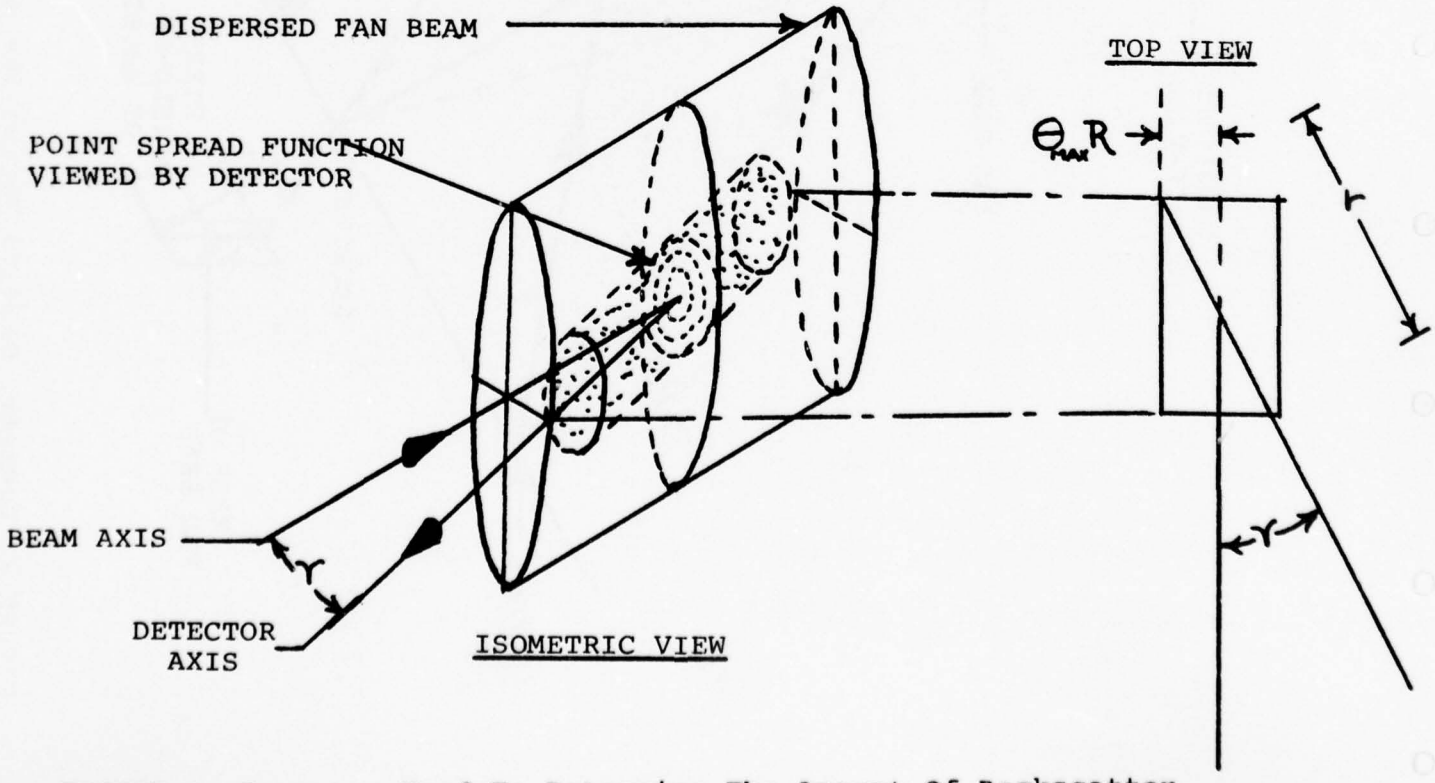

FIGURE 4. Geometry Used To Determine The Amount Of Backscatter

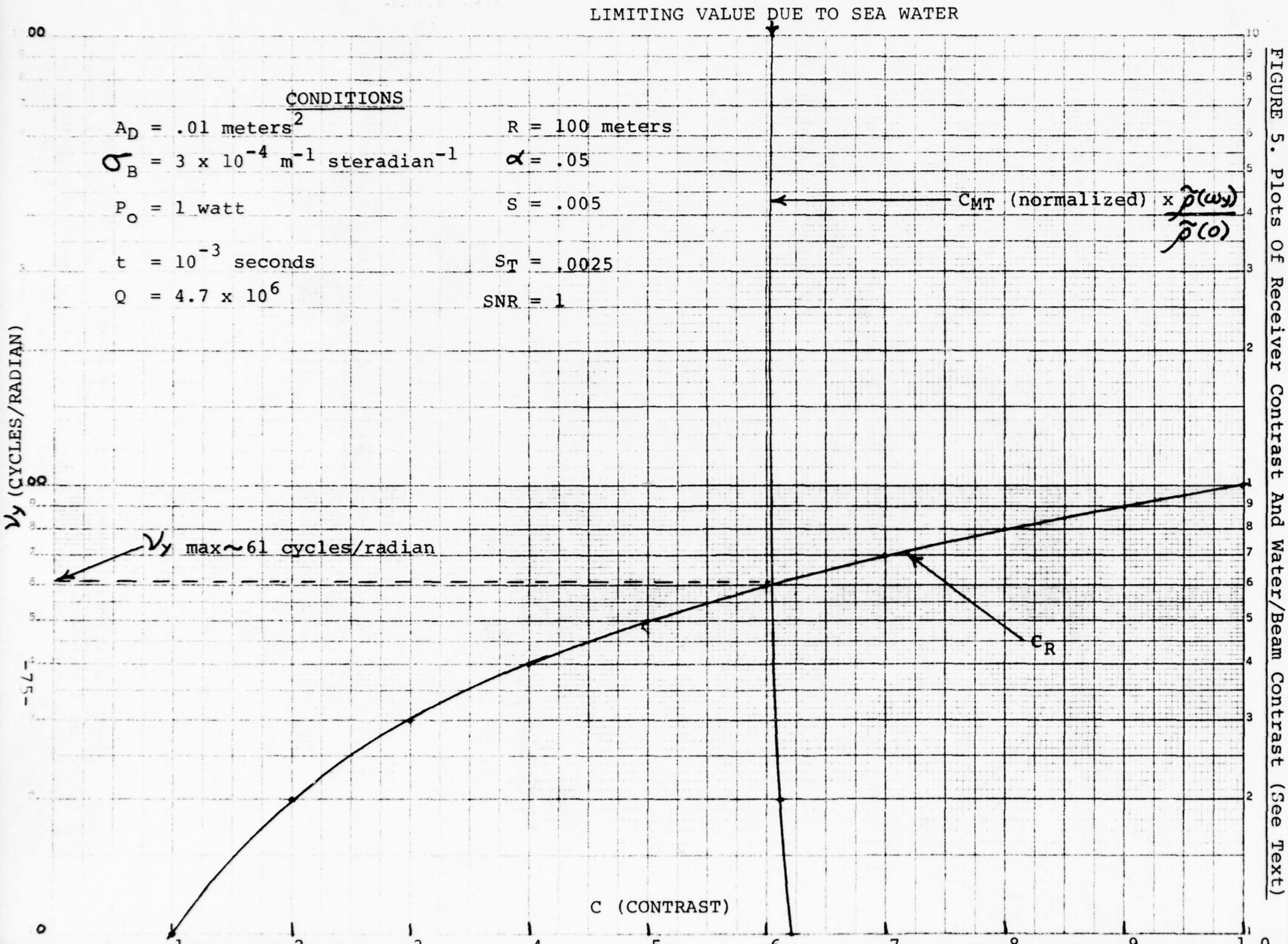

FIGURE 5. Plots Of Receiver Contrast And Water/Beam Contrast (See Text)

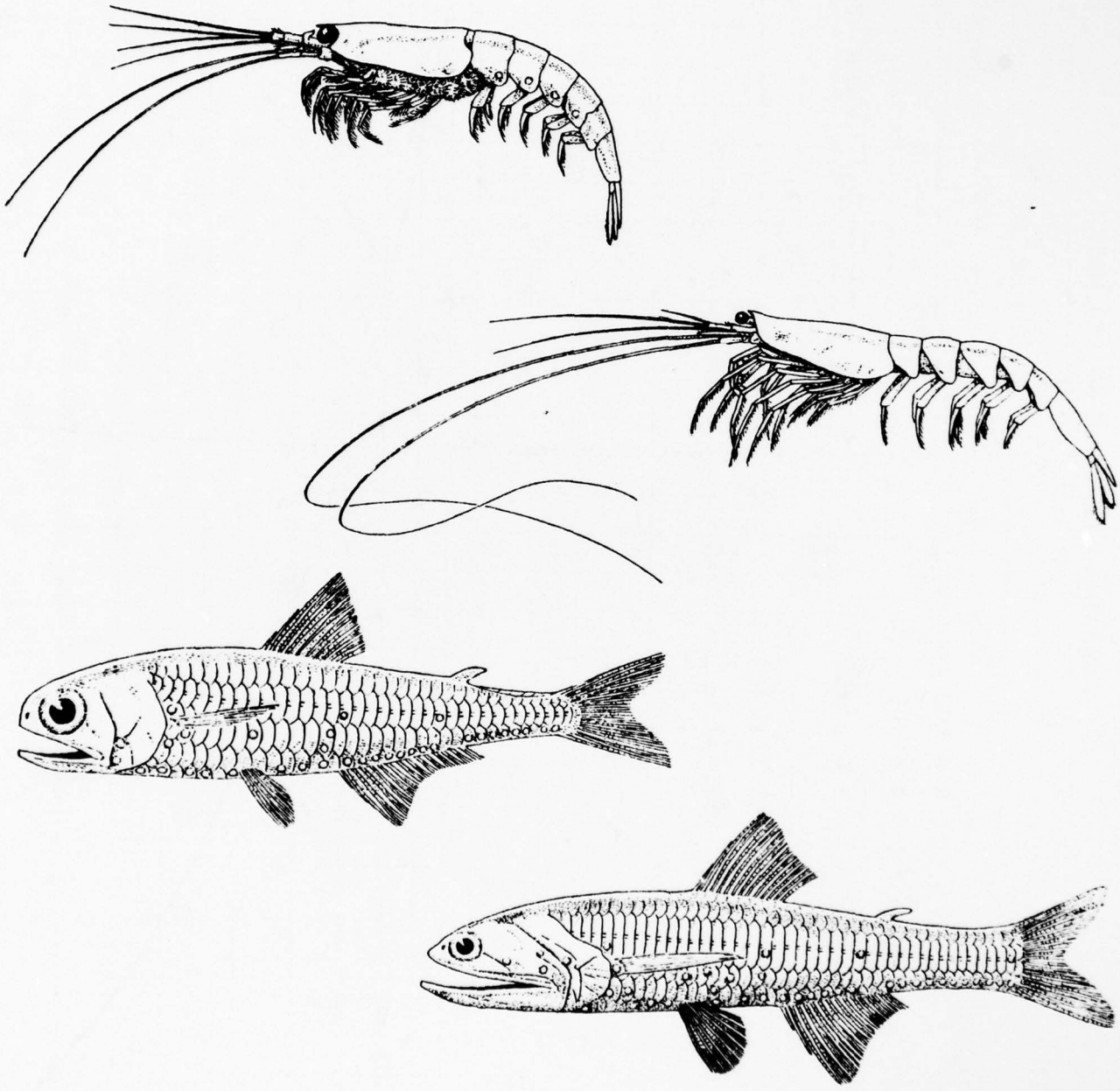

FIGURE 6. SCATTERING-LAYER ORGANISMS include crustaceans and fishes. Among them are (top to bottom) a euphausiid, a sergestid and two forms of myctophids or lantern fish. The animals range in size from about an inch for the euphausids up to three inches for the lantern fish. The four spots on the euphausids and the similar spots on the myctophids are photophores or light-producing organs.

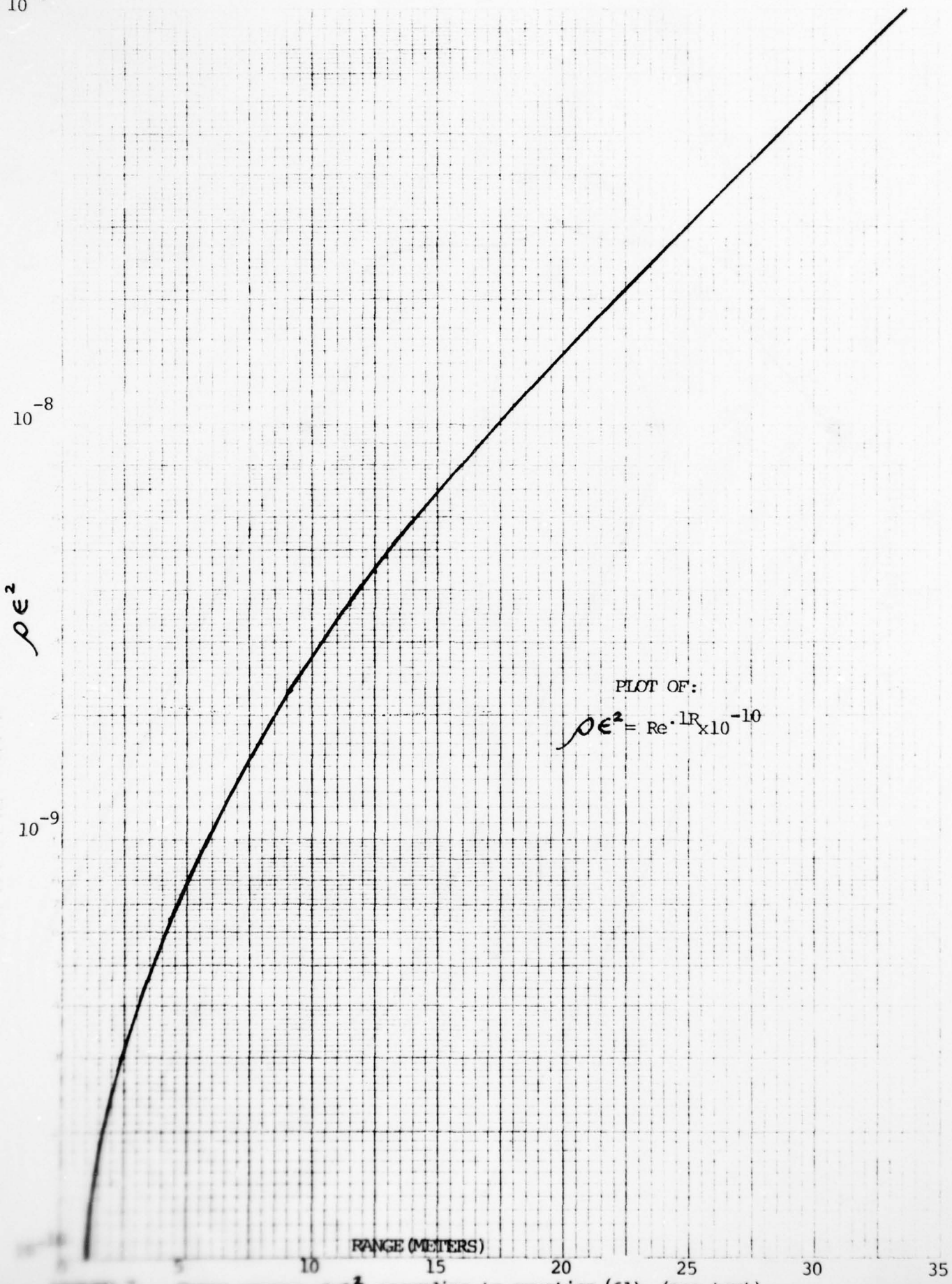

FIGURE 7. Range versus $\rho\epsilon^2$ according to equation (61) (see text).

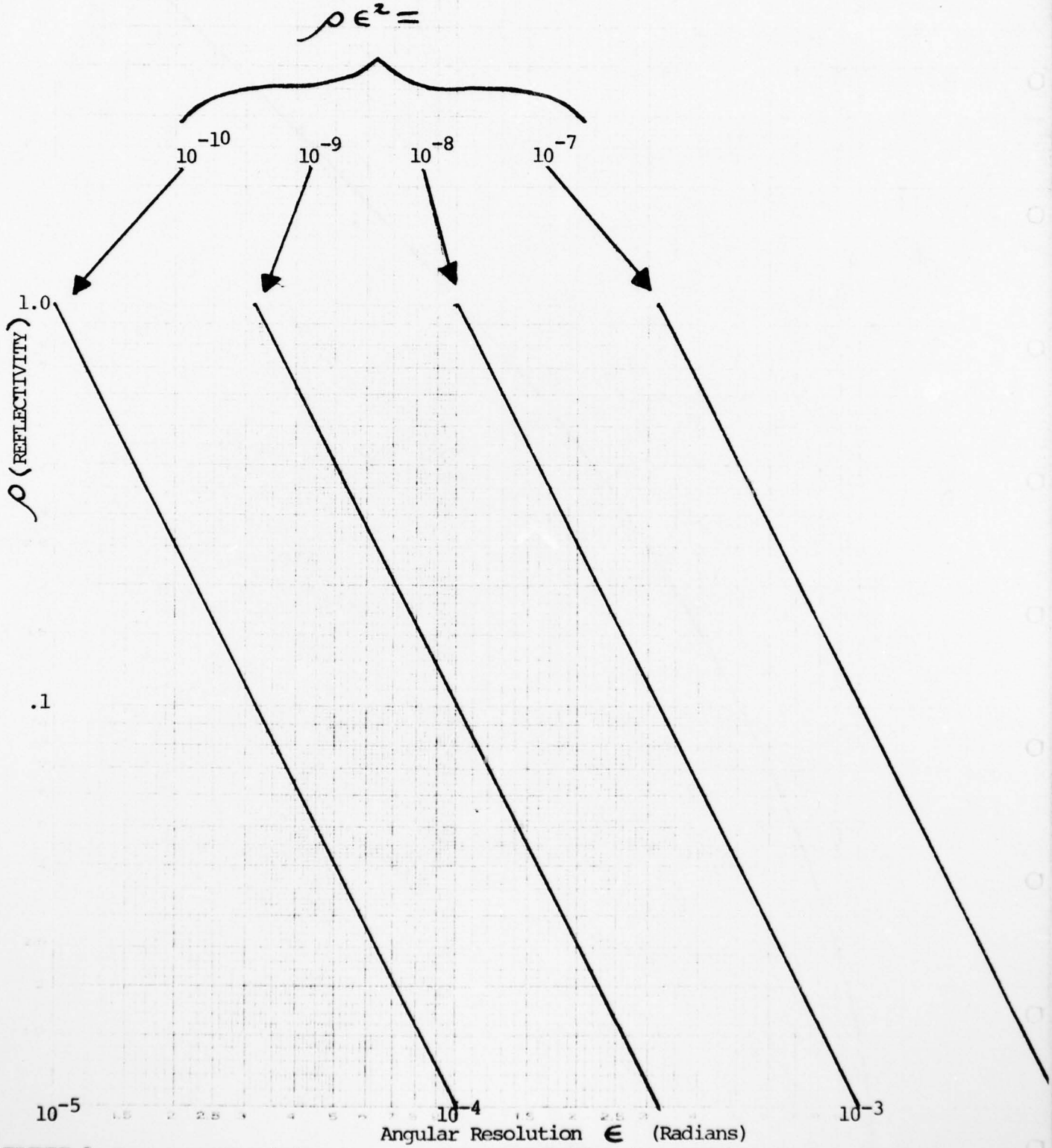

FIGURE 8. Target reflectivity versus angular resolution (see text)

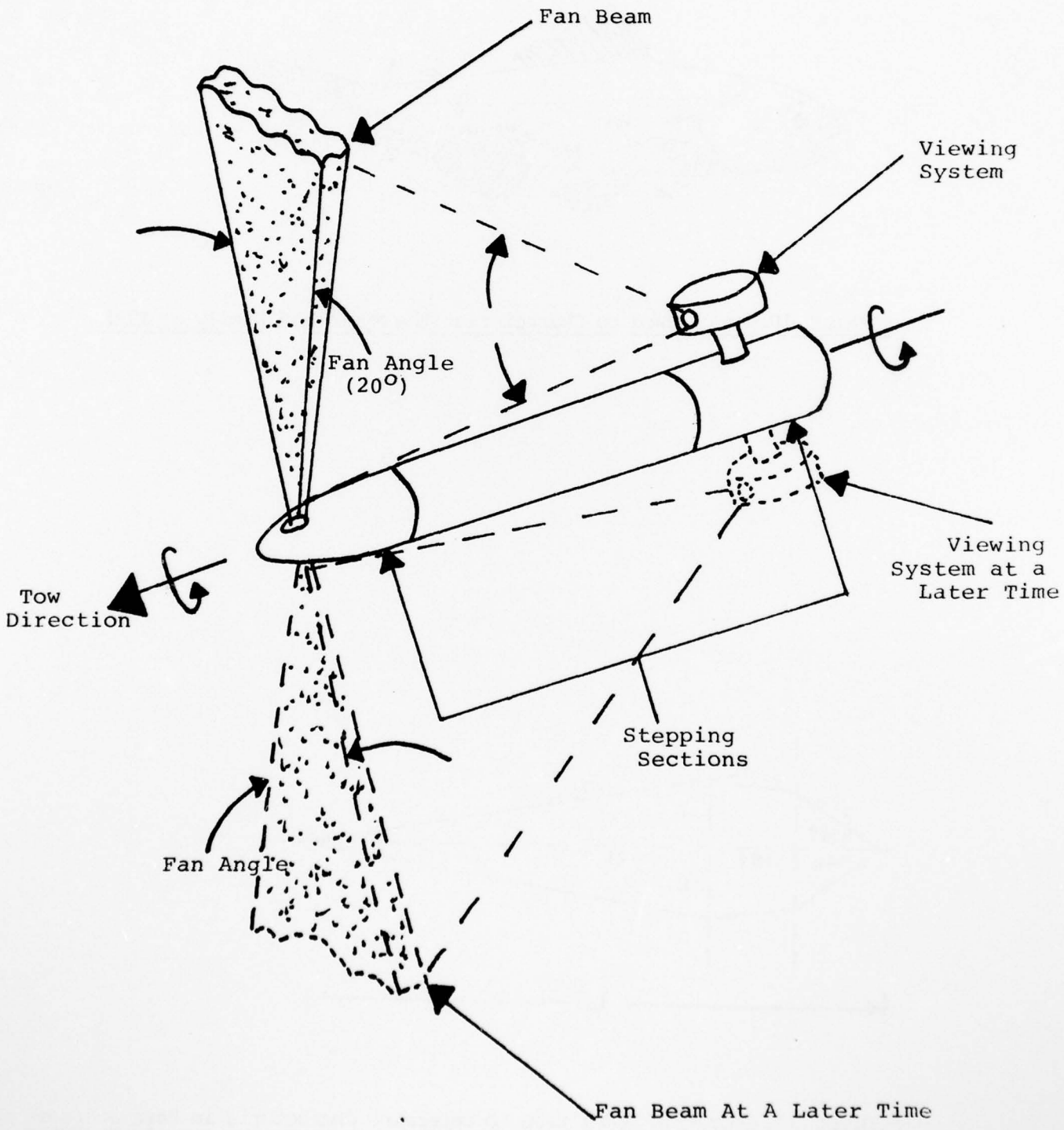

FIGURE 9. Suggested Scanning Configuration for Viewing Mid-Water Nekton (See Text).

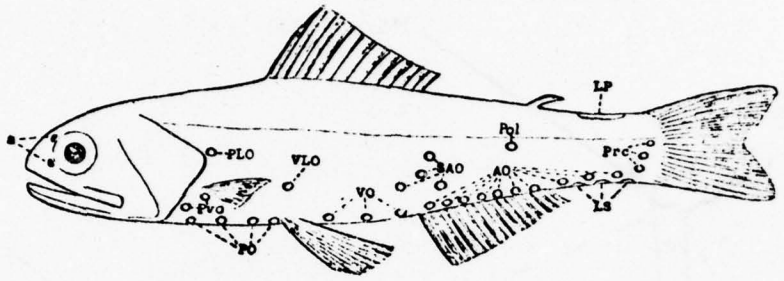

FIGURE 10. Model Used to Characterize the Myctophid Family of Fish

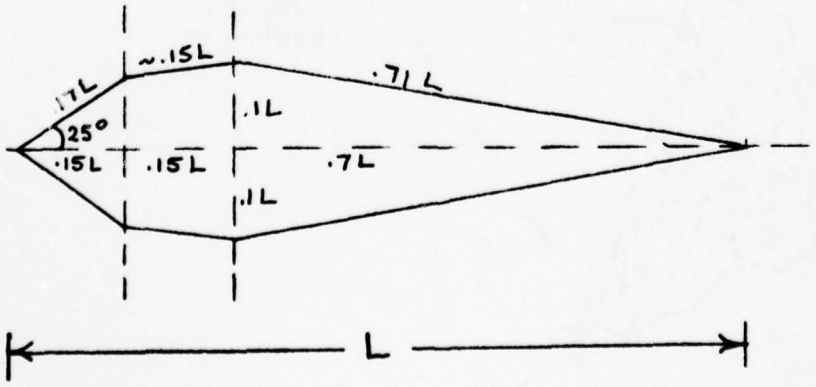

FIGURE 11. Geometric Model Used to Determine Characteristic Parameters of Myctophid Family of Fish

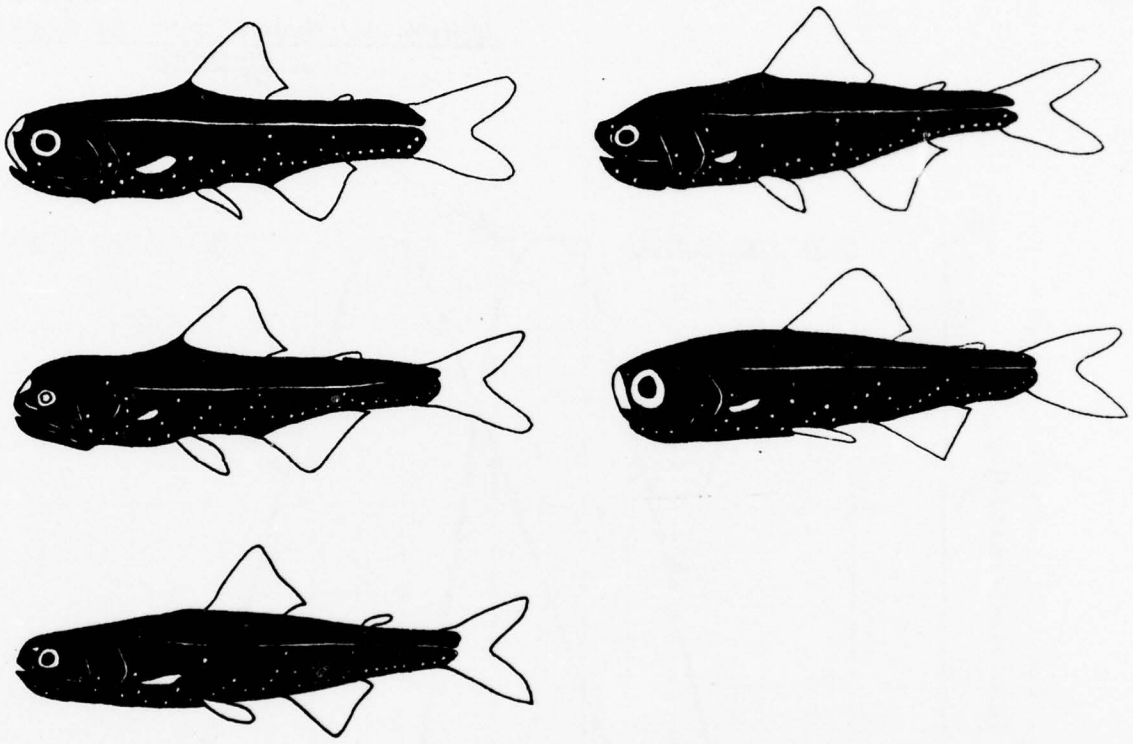

FIGURE 12. The Different Spatial Arrangement Of Photophores In A Closely Related Group Of Lantern Fish of the Genus DIAPHUS. In the left row from top to bottom, DIAPHUS MACROPHUS, DIAPHUS LUCIDUS and DIAPHUS SPLENDIDUS, Right Row, DIAPHUS GARMANI and DIAPHUS EFFULGENS. Each species has developed its own pattern, different from all the rest, which enables a lantern fish to identify other individuals of its own species.

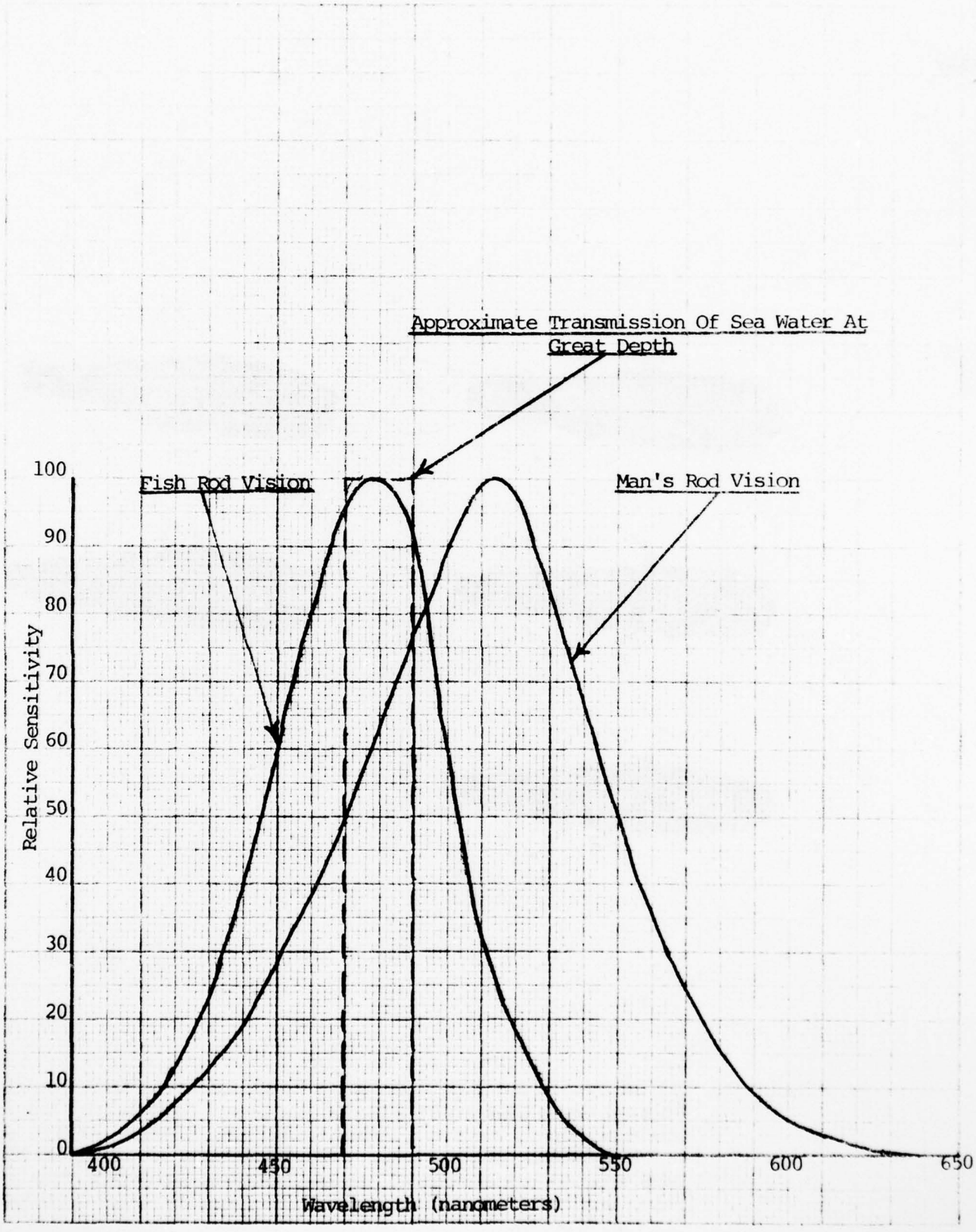

FIGURE 13. Comparison of Fish Vision and Man's Rod Vision

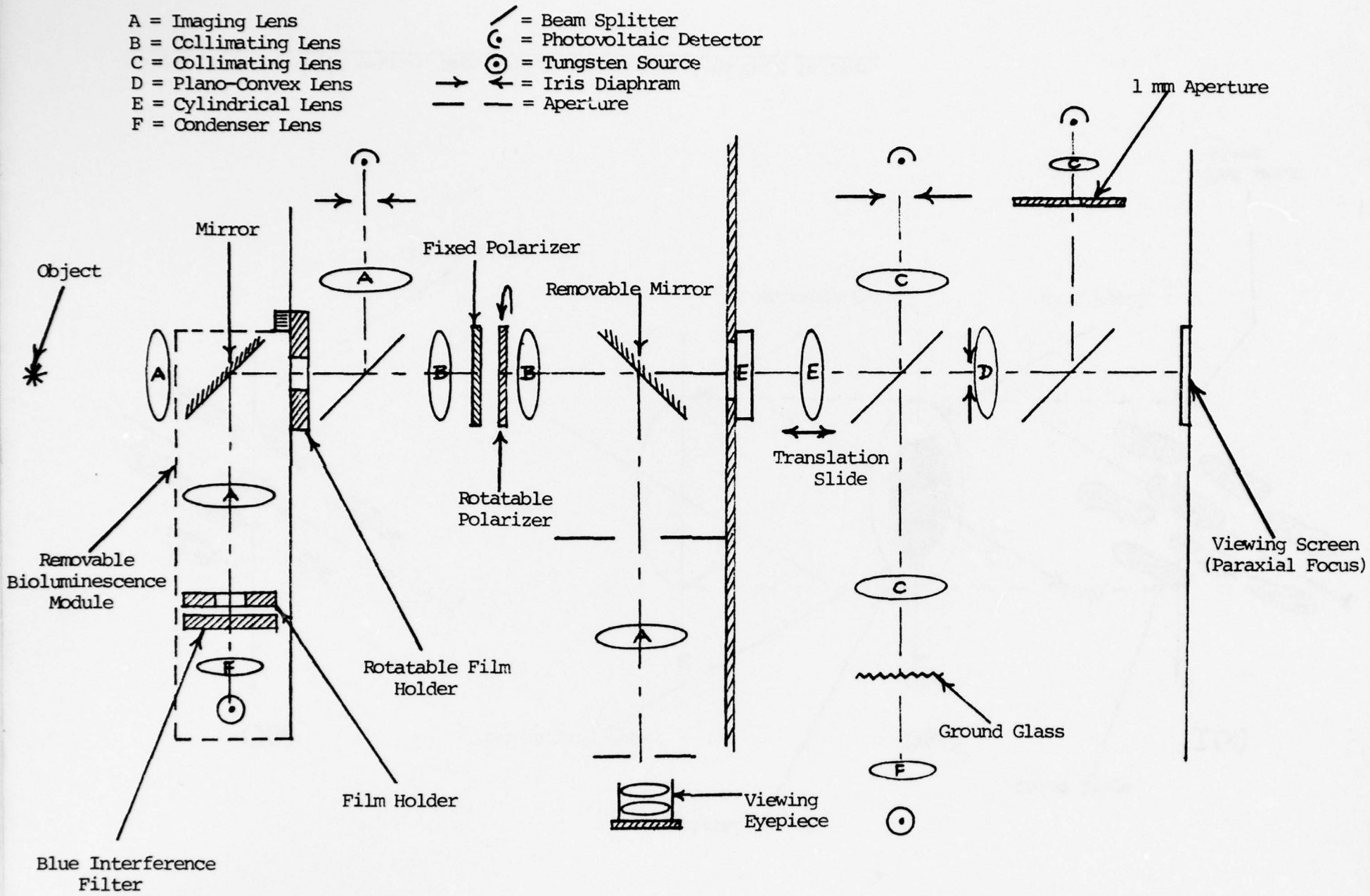

Figure 14.Optical Diagram Of Proposed Optical Simulator Of Image Degradation In Water Viewing Systems (not to scale).

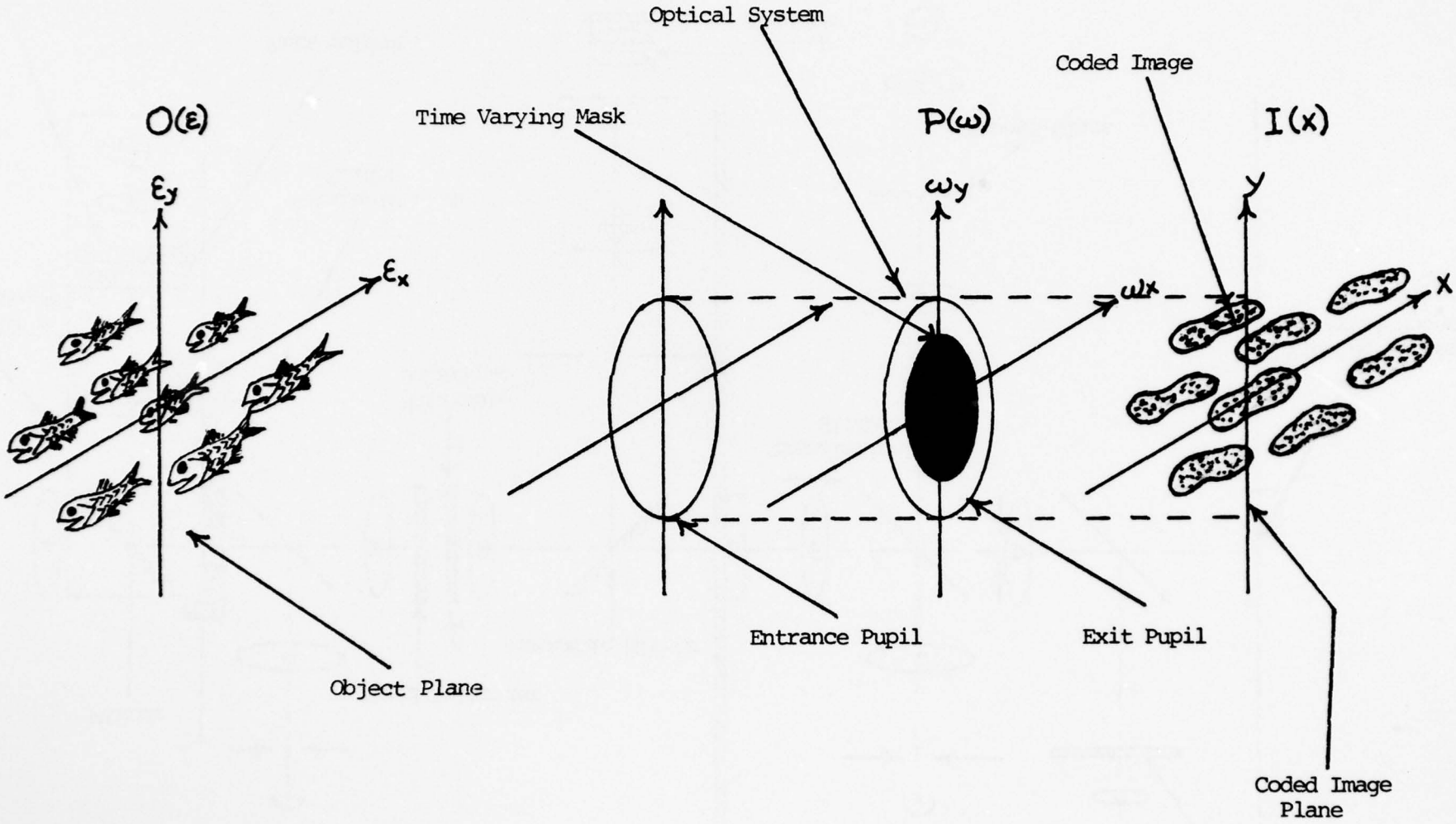

Figure 15. Geometry of Pattern Recognition System Equations Used in Text.

APPENDIX A

RANGE OF ORGANISMS CONSIDERED FOR THE SAMPLING OF THE MICRO- AND MACRO-MESOPELAGIC NEKTON

SCHOOL CHARACTERISTICS

ORGANISM	GENUS/SPECIES	LARVAL SIZE	ADULT MIN.	ADULT MAX.	COLORATION	DEPTH	DENSITY
ELASMOBRANCHS	Somnicsus microcephalus (Large Sleeper or Greenland Shark)	Unknown (Birth)	3-4 m	8 m	Brown to Gray to Black Below and Above	200 - 600 m.	Unknown
	Centroscymnus coelolepis	23 cm. @ birth	--	1.1 m	Dark Brown Above and Below	330 m.	"
	Sphyrna mokarran (Great Hammerhead)	71 cm. @ birth	--	5 m	Gray to Dark Olive Above to Pale Olive Below	?	"
	Carcharodon carcharias (Great White)	127 cm. @ birth	5-6 m	9-12 m	Brown to Gray-Black Above to Dirty White Below	1000 m	"
	Scyliorhinus retifer	7.6 cm @ birth	--	0.7 m	Dark Reddish Brown Above; Yellowish Below	73 - 228m	"
	Pseudotriakis microdon (Atlantic False Cat Shark)	Unknown (Birth)	--	2.9 m	Uniform Dark Brown to Gray	300 - 1476m	"
	Cetorhinus maximus (Basking Shark)	1.5 m @ Birth	--	14 m	Grayish Brown to Gray or Nearly Black Below	?	50-250/ meter^3
	Oxynotus centrina (Humatin)	Unknown (Birth)	--	1 m	Brown, Dark Gray, Reddish Brown	30 - 500m	Unknown
	Dalatius licha (Darkie Charlie)	Unknown (Birth)	--	1.5 m	Chocolate Brown	100 - 1000 meters	"

SCHOOL CHARACTERISTICS (cont'd)

ORGANISMS	GENUS/SPECIES	LARVAL SIZE	ADULT MIN.	ADULT MAX.	COLORATION	DEPTH	DENSITY
Odontoceti							
Delphinidae							
Porpoise	Stenella graffmani	-					Single & mixed species:
	Stenella long irostris	-					"
	Delphinus delphis	-					Greater than 1000 meter^{-3}
Mystacoceti							
Balaenidae	Balaena mysticetus (Right Whale)	-	15	18 m.	Skin: black; Throat/chin-cream colored		?
Eschrichtidae	Eschrichtius glaucus (Gray Whale)	-	10	14 m.	Black or slate with grayish patches of barnacles.		?
Balaenopteri-dae	Balaenoptera physalus (Common Roqual)	-	18	23 m.	Back: Grayish; Underside: White		20-100 meter^{-3}
	Balaenoptera musculus (Blue Whale)	-	24	30 m.	Slate blue		Travels singly

SCHOOL CHARACTERISTICS (cont'd)

ORGANISMS	GENUS/SPECIES	LARVAL SIZE	ADULT MIN.	ADULT MAX.	COLORATION	DEPTH	DENSITY
TELEOSTS (BONY FISHES)							
Gonostomidae	Cyclothone sp.	-	10 -	28 mm.	Pale to Translucent Black	200 - 1500 m.	Unknown
	Vinciguerria attenuata	-	4 - 5 cm.		Silver Sided		"
Myctophidae (Lantern Fish)	Diaphus elucens	-	To 17 cm.		Silver Sided		
	Ceratoscopelus maderensis	-	52 - 73 mm.		Silver Sided	To 1800 m.	1-15/m^3
	M. punctatum	-	To 10 cm.		Silver Sided		Unknown
Sternoptychidae (Hatchet Fish)	Argyropelecus affinis	-	5 - 51 mm.		Silver Sided		"
Gempylidae	Thyrsitops violaceus	-	8 - 195 mm.				"
Melanostomiatidae	Flagellostomias boureei	-	15 - 99 mm.		Black	To 4500 m.	"
Searsidae	Persparsia taningi	-					
Opisthoproctidae	Rhynchohylus	-	20 - 30 mm.		Silvery + Dark Spots	200 - 600 m.	"
Paralepididae	Sudis hyalina	-	1 m.			To 600 m.	"
Alepisauridae	Alepisaurus ferox Lowe	-	1 m.		Silver Sided	400-600 m.	"
Nemichthyidae (Snipe Eels)	Nemichthys scolopacea	-	2 m.			To 1800 m.	"
Scombridae (Tuna, tunny, bonito, albacore, mackrel)	Thunnus thynnus L.	-	To 2 m.		Dark Metallic Blue/Greenish Sheen; Silver Bars on Side; White Belly	To 180 m.	25/m^3

SCHOOL CHARACTERISTICS (cont'd)

ORGANISMS	GENUS/SPECIES	LARVAL SIZE	ADULT MIN.	ADULT MAX.	COLORATION	DEPTH	DENSITY
CEPHALOPODS (SQUID)	Ommastrephes illecebrassa	-	20-30 cm.		Black, brown and reddish yellow pigment in chromatophores of skin		Unknown
	Loligo peali	-	30-46 cm.				
	L. opalescencs	-	30 cm.				
	Architeuthis sp.	-	15 m.				
	Dosidicus gigas	1.2 - 9.5 mm	0.6-1.8 m. (Mantle)				
(OCTOPUS)	Bolitaena sp.	-	2-5 cm.		Often Transparent	600 - 1500 m.	"
	Amphitretus pelagicus	-	5-6 cm.			250 m.	"
	Cirroteuthis muelleri	-	25 cm.			400 - 3000 m.	"
EUPHAUSIIDS	Euphausia superba	-	4-6 mm.				To 10^8 $meter^{-3}$
PHYSONECTS (Colonial Hydrozoan Jellyfish)	Nanomia bijuga Large Form	-	60 - 70 cm.			200 - 400 m.	300-1000 $meter^{-3}$
	Smaller Form	-	20 - 40 cm.				
	Small Form	-	20 - 30 cm.				
AMPHIPODS (Water Fleas)		-				10,000 m.	
SERGESTID PRAWNS	Sergestes smilis	-	8 - 9.5 mm. (Carpace Length)				

Note: All nekton appear to have positive phototropism except the Myctopidae.

PROFILE OF MESOPELAGIC ORGANISMS IN N.E. TROPICAL PACIFIC DETERMINED WITH A TUCKER O/C TRAWL AT 270-350 M. (21,035 M^3 FILTERED)*

CRUISE: MINOX 3 DATE: 28 OCTOBER 1973

STATION: 8 - TRANSITION FRONTAL HAUL: 36

GEAR: TUCKER O/C TRAWL

HAUL:

DURATION: START - 1509; FINISH - 1657; TOTAL - 108 MINUTES

SAMPLING:

TIME: OPEN - 1528; CLOSE - 1643; TOTAL - 75 MINUTES

MAXIMUM:

WIRE OUT: - M ; SAMPLING INTERVAL: 270 - 350 M.

SAMPLING:

SPEED: 2.25 KNOTS (70.1 M/MIN); VOLUME FILTERED: 21,035 M^3

ORGANISMS	TOTAL COUNT
FISHES:	
MYCTOPHIDS	29
CYCLOTHONE	8
VINCIGUERRIA	247
FRAGMENTS	2
OTHERS:	
COPEPODA	20,246
AMPHIPODA	4
PENAEIDA	37
EUPHAUSIACEA (ADULTS)	1,393
OSTRACODA	1
STOMATOPODA	3
CEPHALOPODA	1

*VENT, R.J. and G.V. Pickwell, Acoustic Volume Scattering Measurements With Related Biological and Chemical Observations in the Northeastern Tropical Pacific (U) NUC TP 525, Naval Under Sea Center, San Diego, California 92132 (1976).

AD-A062 755 GENERAL SENSORS INC FORT WASHINGTON PA F/G 8/1
STUDY OF THE FEASIBILITY OF USING AN ADVANCED OPTO-ELECTRONIC I--ETC(U)
NOV 78 H SADJIAN N00014-77-C-0344
UNCLASSIFIED 6S-1-78-ONR NL

2 OF 2
AD A062755

END
DATE FILMED
3-79
DDC

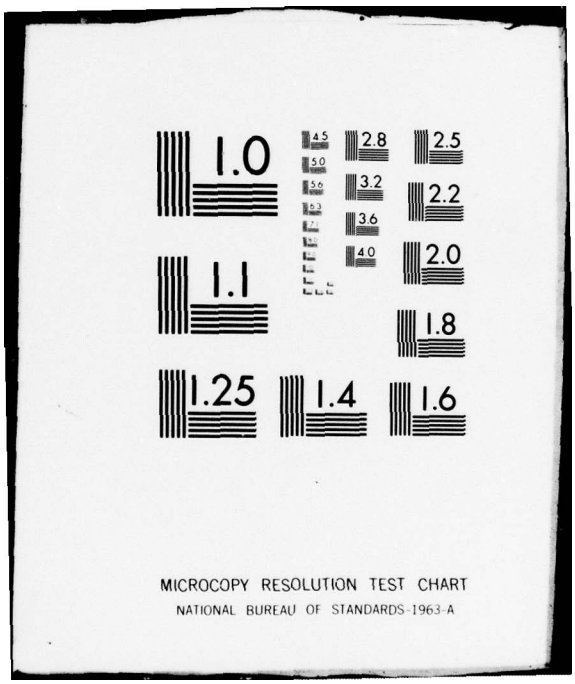
1.0
1.1
1.25
1.4
1.6
1.8
2.0
2.2
2.5
2.8
3.2
3.6
4.0
4.5
5.0
5.6
6.3
MICROCOPY RESOLUTION TEST CHART
NATIONAL BUREAU OF STANDARDS-1963-A

COLORATION OF MESOPELAGIC NEKTON AND RELATED ORGANISMS

PLANKTON		
	COPEPODS ARROW WORMS SIPHONOPHORES	TRANSLUCENT/ TRANSPARENT
MEDUSAE	AGLISCRA IGNEA	FLAMING RED
NEMERTEAN WORMS		REDDISH
ARROW WORMS	SAGITTA MACROCEPHALA EUKROHINA FOWLERI	SPECKLED OR SUFFUSED WITH RED PIGMENTS
COPEPODS	GAETANUS	RED
OSTRACODS	GIGANTOCYPRIS	RED & ORANGE
PRAWNS	ACANTHEPHYRA SYSTELLASPIS	SCARLET
CEPHALOPODS	MASTIGOTEUTHIS HISTIOTEUTHIS	RED
WHALE-FISHES		RED OR PLUM
CYCLOTHONE	C. SIGNATA C. BRAVERI	PALE OR TRANSLUCENT
GONOSTOMIDAE	VINCIGUERRIA	SILVER SIDED FISH
STERNOPTYCHIDAE	HATCHET FISH	SILVER SIDED FISH
MYCTOPHIDAE	LANTERN FISH	SILVER SIDED FISH
ASTRONESTHIDAE	STAR EATERS	DARK COLORED FISH ARMED WITH LONG, SHARP TEETH
MELANOSTOMIATIDAE	DRAGON FISHES	DARK COLORED FISH ARMED WITH LONG, SHARP TEETH
MALACOSTEIDAE	RAT TRAP FISHES	DARK COLORED FISH ARMED WITH LONG, SHARP TEETH
CHIASMODONTIDAE	GIANT SWALLOWERS	DARK COLORED FISH ARMED WITH LONG, SHARP TEETH

CHARACTERISTICS OF MYCTOPHID FISH (Ceratoscopelus Maderensis) DETERMINED IN SLOPE WATER BY THE DEEP SUBMERGENCE VEHICLE ALVIN'S ECHO-RANGING SONAR*

LOCATION OF STUDY	South of Woodshole, MA 30° 48'N, 70° 33'W
DEPTH	To 1800 m.
ECHO SOUNDER CHARACTERISTICS	Discrete hyperbolic echo-sequences at 12 KHz (Midday Depth); 3 KHz at 30 m.
TARGET IDENTIFICATION	Captured by driving Alvin through school.
FISH SIZE	$\bar{X}$ = 62.4 mm SD = 2.9 mm RANGE = 52 -73 mm
COMPUTATION OF NO. TARGETS	
VOLUME SEA WATER	23.76 X 10^5 m^3
FISH DENSITY	10-15/ m^3 water
FISH SCHOOL DIMENSIONS	
THICKNESS	5 - 10 m
DIAMETERS	10 - 100 m
DISTANCE APART	100 - 200 m
ATTITUDE IN WATER	Fish at rest, motionless, horizontal or slightly oblique, random orientation.
RESPONSE OF FISH TO APPROACHING ALVIN	Moved down and away; fish moved more rapidly in shallow water than deep water.
RESPONSE TO LIGHT (TUNGSTEN)	Rapidly swam away (negative phototropic response).

*After Science, 160, 991-993 (1968).

APPENDIX B

DATA TRANSMISSION ANALYSIS

This analysis is for the case of a fan beam scanned back and forth producing a pyramid shaped volume as shown in figure B-1. The volume of the pyramid is 1/3 S^2R consisting of frames of Ne sides where N is the number of photodiodes in a linear array and e the resolution length. It is assumed that the depth separation between frames is 10e. In addition, there are N^2 elements/frame and there are 10eR frames per pyramid volume. If we assume an e = .1 meters at 100 meters and an N = 50, then the volume of the pyramid is about 833 $meters^3$, there are 2500 elements per frame and there are 100 frames per volume.

For the purposes of this analysis, we will assume that a Reticon 50x50 photodiode array is used for recording which has a worst case scan rate of $5x10^4$ elements/sec. or $20x10^{-6}$ sec./elements. The electronics are considered at this rate. Selected arrays may be faster and optical candidates may be lower. Either direct video (analogue) or digital cable transmission is possible.

1. Analogue Transmission

The block diagram of the system with analogue data transmission is shown in figure B-2. The basic element clock is enabled by the synchronous signal from the fan beam. The x and y registers are internal to the array. A composite video is created as a result. Using the above limitations on speed, the following characteristics are arrived at:

Levels of grey	16
Elements/Volume	$2.5x10^5$
Element speed	$5x10^4$/sec.
Transmission Efficiency	92%
Allowable cable atten.	5.75 db @ 100 KHz
Frame speed	18.5/sec.

Since a typical cable length might be 10,000 ft., this means an attenuation of .57 db/Kft. @ 100 KHz. This would appear to require a steel jacketed, coaxial cable. An example is US Steel's 2569RC with an attenuation of .55 db/Dft. @ 100 KHz. A shorter cable would allow relaxation on the characteristics. Note that element speed cannot be increased and the cable is limiting. The transmission efficiency above is due to the short time for the end of line and end of frame pulses. It is possible that additional time will be needed for the fan beam to start and stop.

The above cable is 0.7" in diameter and weighs 700 lb./Kft. It would be a major cost factor. If a less costly cable were desired, a 2J42RC might be selected. This would give a 1.1 db/Kft. @ 100 KHz and would require a reduction in element speed.

2. Digital Transmission

The electronics are somewhat different from the analogue case. A block diagram of a suggested arrangement for digital transmission is shown in figure B-3. A bit rate clock operates at 5x the element speed. A 4 bit data rate (16 levels of grey) are used and formulated as follows:

start bit	(1)
word 1	4 bits
word 2	4 bits
stop bit	(0)

This would be a total of 10 bits with 8 bits of data and 2 words. The total transmission efficiency is 2499x4 bits in 2500x5 bits or 79.96%. The system characteristics are:

Levels of grey	16 (4 bit)
Elements/volume	2500
Element speed	5×10^4
Transmission Eff.	80%
Allowable Cable Atten.	3 db
Frame speed	16/sec.

3. Cables

Cables for structural and data transmission are manufactured by US Steel, Rochester Cable, Victor Cable Co., etc. Examples for US Steel are:

Manufacturer	#	Dia.(in.)	Break Pt. (lbs.)	Wt.(lbs./Kft.)	Attn.	Element Speed (Analogue)	Frame Speed (Sec^{-1})
US STEEL	2J69RC	.686	34,000	704.0	.55	51.5	19
"	2H52RC	.528	20,000	472.0	1.0	31.0	11.5
"	2J42RC	.420	13,300	272.0	1.1	31.0	11.4
"	2H38RC	.381	12,600	237.0	1.3	26.6	9.8
"	2H30SC	.298	6,700	133.0	1.9	17.7	6.5

For digital transmission, the element speed will be 0.45 of the above and the frame speed even lower.

4. Conclusions

For the pyramid scan, the cable would appear to be the important limitation for a maximum data rate. Analogue data transmission gives approximately twice the frame speed of the digital transmission. Using the cable examples shown above, we have that,

	Attenuation	Analogue Transmission			Digital Transmission		
No.	(db/Kft. @ 100KHz)	Element Speed (KHz)	Frame Speed (Hz)	Time/ 100 Frames (sec.)	Element Speed (KHz)	Frame Speed (Hz)	Time/ 100 Frames (sec.)
1	.55	51.5	19.0	5.3	23.4	7.5	13.3
2	1.1	31.0	11.4	8.8	14.0	4.5	22.2
3	1.3	26.6	9.8	10.2	12.1	3.9	25.6
4	1.9	17.7	6.5	15.4	8.0	2.6	38.4

Hence the worst case of 5×10^4 for the element scan would appear to be consistent. The sample rate above is also the A/D converter rate. High speed 8 bit A/D converters are capable of conversions at 1 MHz and therefore are by no means limiting.

5. Additional Comments For The Pyramid Shape Scan

For the examples shown, the time/volume varies from 5.3 sec. to 38.0

sec. At a tow speed of 1 knot (½ meter/sec.), the separation of source and viewing system, l_I, varies from 2.6 meters to 19.2 meters. In the first case, overlapping occurs and in the second a gap exists. It would appear that some consideration should be given to circular scanning for more optimum coverage. As shown in the previous sections, circular scanning also is required to meet some of the resolution and sampling area criteria.

If we define the efficiency of coverage as proportional to the volume seen unduplicated to what could be seen, then we have that,

$$(\text{Efficiency}) = \frac{1/3\ RS^2}{RL_IS} \qquad \text{for } L_I \text{ greater than } S$$

$$= \frac{1/3\ RS^2 \quad - \tfrac{1}{2}(S-L_I)^2R}{RL_IS} \qquad \text{for } L_I \text{ less than } S$$

Additionally, if T_v is the time/volume and u is the tow speed, then L_I is $T_v$xu. If we assume a tow speed of u = 1 knot, then we have that,

Time/Volume (sec.)	Coverage Efficiency (%)
4	38.3
6	42.2
8	39.1
10	33.3
20	16.6
40	8.3

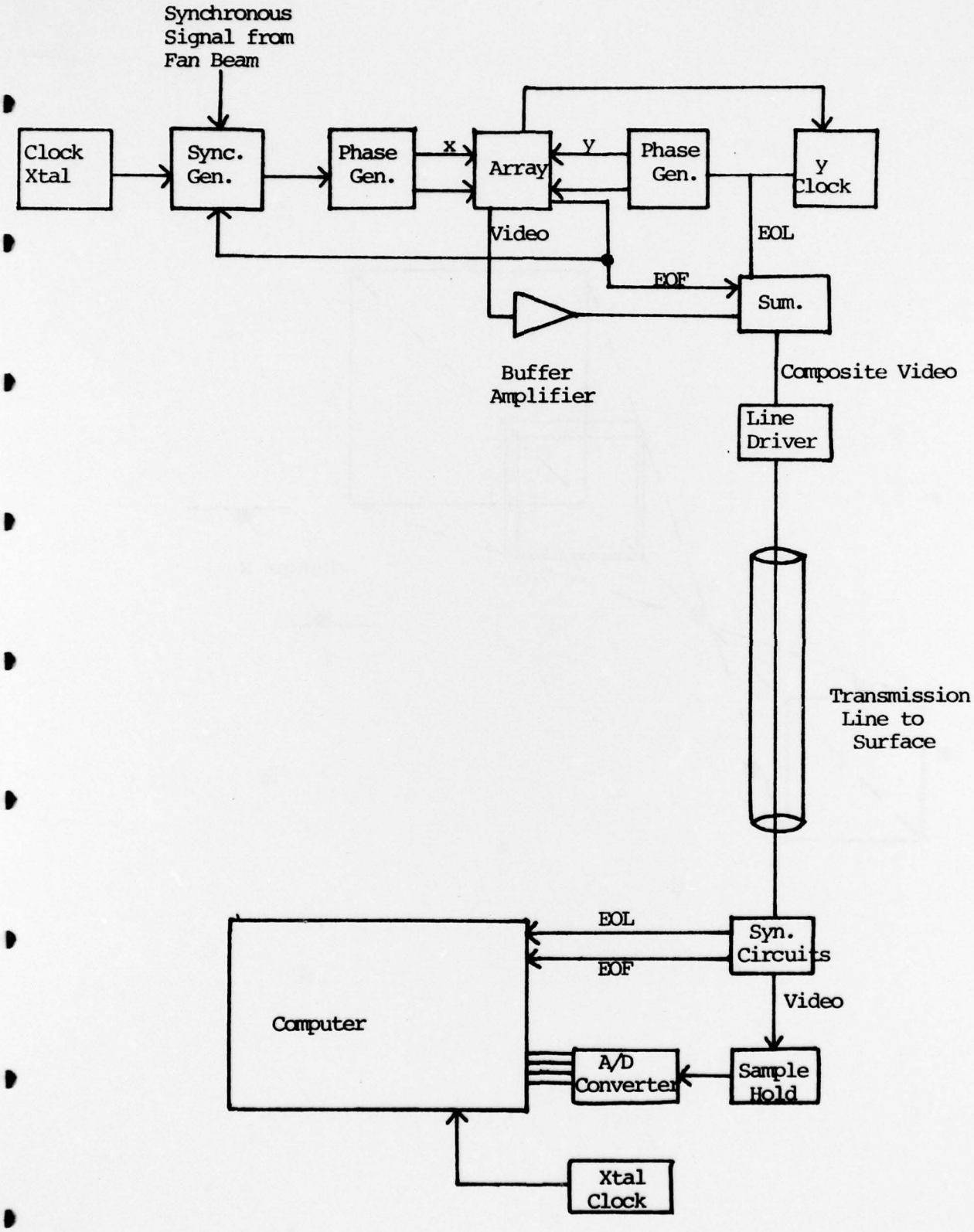

Figure B-2. Example Of Block Diagram Of A System With Analogue Transmission

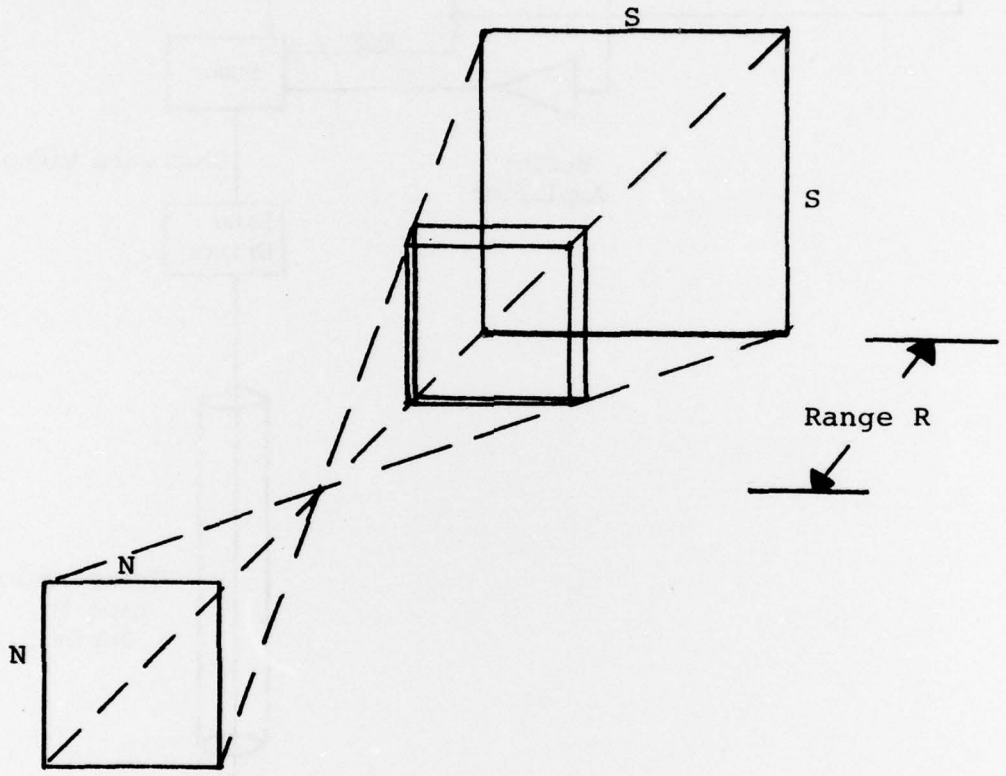

Figure B-1.Geometry Used To Analyze Data Transmission From Pyramid Scan

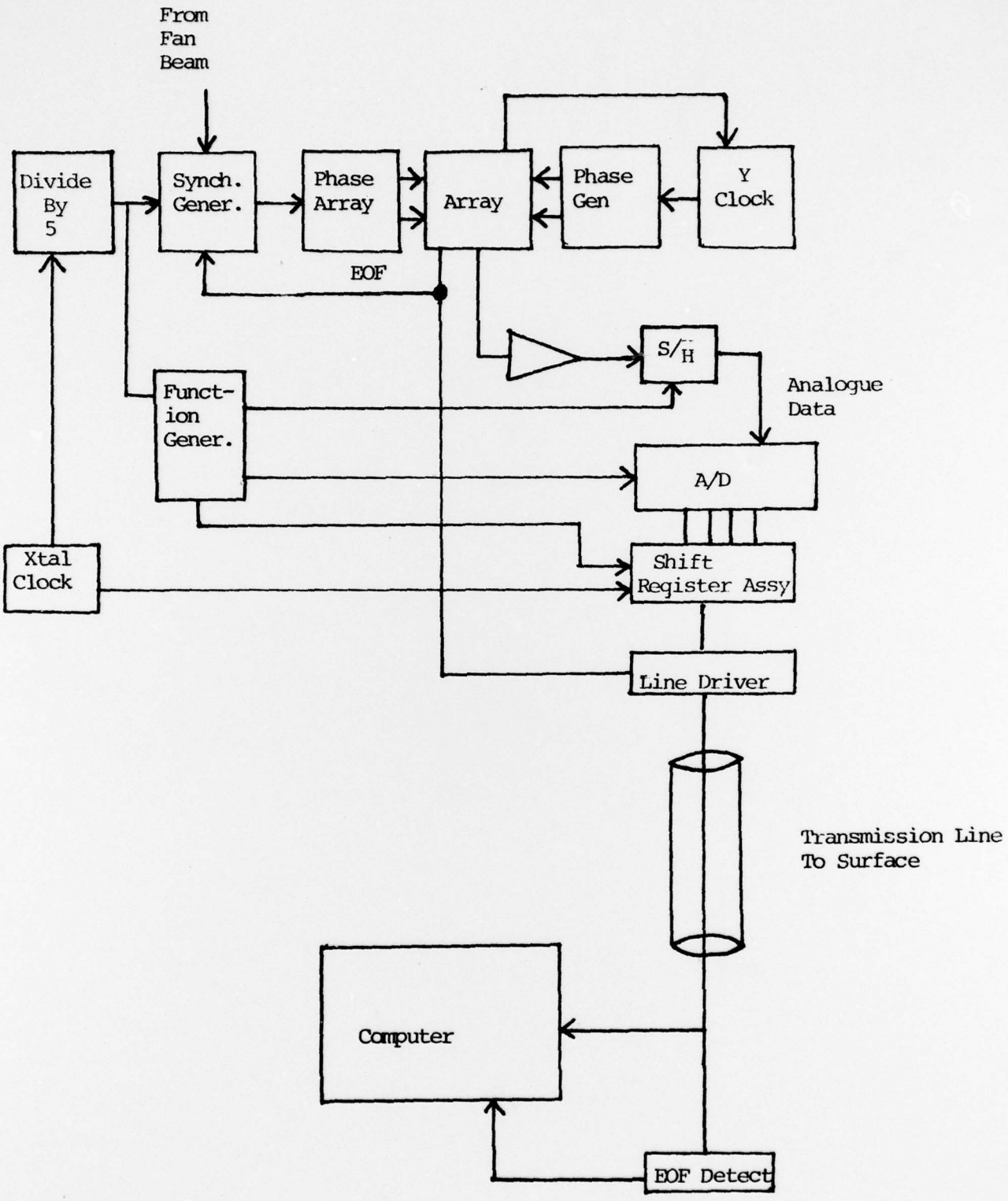

Figure B-3. Example Of Block Diagram Of A System With Digital Transmission

APPENDIX C

SELECTED BIBLIOGRAPHY

ON MID-WATER NEKTON

1. ATSTATT, Lenora H. and Roger R. Seapy, An Analysis of Sampling Variability in Replicated Midwater Trawls Off Southern California, J. Exp. Mar. Biol. Ecol., 14, 261-273 (1974).

2. A Glossary of Ocean Science and Undersea Technology Terms, L. M. Hunt and D.G. Groves, Ed., vii, 173 pgs., Compass Publications, Inc., Arlington, Virginia (1965)

3. A List of Common and Scientific Names of Fishes from the United States and Canada, Edition 3, 150 pgs., American Fisheries Society, Special Publication No. 6, Washington, D.C. (1970).

4. BACKUS, R.H.,J.E. Craddock, R.L. Haedrich and D.L. Shores, Mesopelagic Fishes and Thermal Fronts in the Western Sargasso Sea, Marine Biology, 3, 87-106 (1969).

5. BACKUS, R.H., J.E. Craddock, R.L. Haedrich, D.L. Shores, J.M. Teal, and A.S. Wing, Ceratoscopelus Maderensis: Peculiar Sound-Scattering Layer Identified With This Myctophid Fish, Science, 160, 991-993 (1968

6. BACKUS, R.H., J.E. Craddock, R.H. Haedrich, and D.L. Shores, The Distribution of Mesopelagic Fishes in the Equitorial and Western North Atlantic Ocean, p. 20-40, in Proc. Int. Sym. Biol., Sound Scattering Ocean, Maury Center Rep. 005, G. Brooke Farquahr, ed., April (1970).

7. BADCOCK, J., and N.R. Merret, Midwater Fishes in the Eastern North Atlantic - I; Progress in Oceanography, 7 (1), 3-58 (1976).

8. BADCOCK, Julian, Colour Variation in Two Mesopelagic Fishes and Its Correlation With Ambient Light Conditions, Nature, 221, 383-385 (1969)

9. BARHAM, Eric G., Siphonophores and the Deep Scattering Layer, Science, 140, 826-828 (1963).

10. BARHAM, Eric G., Deep Scattering Layer Migration and Composition: Observations From a Diving Saucer, Science, 151, 1399-1403 (1966).

11. BARHAM, E.G., Deep-Sea Fishes, Lethargy and Vertical Orientation, p. 100-118, In Proc. Int. Symp. Biol. Sound Scattering, G. Farqu Maury Center Report 005 (1971).

12. BARNES, A.T. and J.F. Case, The Luminescence of Lantern Fish (Myctophidae): Spontaneous Activity and Responses to Mechanical, Electrical and Chemical Stimulation, J. Exp. Mar. Biol. Ecol., 15, 203-221 (1974)

13. BUTLER, John L. and Elbert H. Ahlstrom, Review of the Deep Sea Fish Genus Scopelengys (Neoscopelidae) With a Description of a New Species, Scopelengys Clarkei, From the Central Pacific, Fishery Bulletin, 74, No. 1 (1976).

14. CASEY, John G., Anglers' Guide to Sharks of the N.E. United States, Maine to Chesapeake, Bureau of Sport Fisheries and Wildlife Circular No. 179, 32 p. (1964).

15. CHINDONOVA, Yu. G. and N.I. Kashkin, Comparison of the Biological and Acoustic Methods of Assessing Sound-Scattering Layers, Oceanology, 9, 430-439 (1969).

16. CLARKE, Malcom R., New Technique for the Study of Sperm Whale Migration, Nature, 238, 405-406 (1972).

17. CLARKE, T.A., Some Aspects of the Ecology of Lantern Fishes, (Myctophidae) in the Pacific Ocean Near Hawaii, Fish. Bull. U.S., 71, 401-434 (1973).

18. CLARKE, T.A. and P.J. Wagner, Vertical Distribution and Other Aspects of the Ecology of Certain Mesopelagic Fishes Taken Near Hawaii USA, U.S. Ntl. Mar. Fish Serv. Fish Bulletin, 74, (3) 635-645 (1976).*

19. COUSTEAU, Jacques-Yves and Phillipe Diole, The Whale, 304 pgs, Doubleday, Inc., Garden City, New York (1972).

20. DAVIES, I.E. and E.G. Barham, The Tucker Opening-Closing Micronekton Net and Its Performance in a Study of the Deep Scattering Layer, Marine Biology, 2, 127-131 (1969).

21. DEES, Lola T. , Cephalopods: Cuttlefish, Octopuses, Squids, Fishery Leaflet 524, U.S. Department of the Interior, Fish & Wildlife Service, Bureau of Commercial Fisheries, Washington, D.C. (1961).

22. DENTON, E.J., J.B. Gilpin-Brown, and P.G. Wright, The Angular Distribution of the Light Produced by Some Mesopelagic Fish in Relation to Their Camouflage, Proc. R. Soc. London, B., 182, 145-158 (1972).

23. DONALDSON, Henry A. and William G. Pearcy, Sound-Scattering Layers in the Northeastern Pacific, J. Canada Fisheries Research Board, 29, (10), 7 pages (1972).*

24. HAEDRICH, R.L. Identification of Deep-Sea Mooring Cable Biter, Deep Sea Res., 12, 773-776 (1965).

25. HALLIDAY, R.G. and W.B. Scott, Records of Mesopelagic and Other Fishes From the Canadian Atlantic With Notes on Their Distribution, J. Canada Fisheries Research Board, 26 (10), 2691-2702 (1969).

26. HERRING, P.J. and M.R. Clarke, Deep Oceans, 320 pgs., Praeger Publishers, New York, New York (1971).

27. Identification and Enumeration of Nekton in Mesopelagic Waters, Computerized Literature Search From Oceanic Abstracts, 13 pgs., 102 Citations, Conducted by Documentation Associates, Los Angeles, California for Environs Systems, Inc., Exton, Pennsylvania (1977).

28. Identification and Enumeration of Nekton in Mesopelagic Waters, Computerized Literature Search From NTIS, 8 pgs., 10 Citations, Conducted by Documentation Associates, Los Angeles, California for Environs Systems, Inc., Exton, Pennsylvania (1977).

29. Identification and Enumeration of Nekton in Mesopelagic Waters, Computerized Literature Search From BIOSIS, 94 pgs., 250 Citations, Conducted by Documentation Associates, Los Angeles, California for Environs Systems, Inc., Exton, Pennsylvania (1977).

30. KASHKIN, N.I. Identification of Sound-Scattering Layers from the Size Structure of the Population of Mesopelagic Sound-Scattering Fish Species, Oceanology, 14 (5), 736-739 (1975).

31. KASHKIN, N.I. On the Quantitative Distribution of the Lantern Fishes Myctophidae in the Atlantic Ocean, Pelagic and Bathypelagic Fishes of the World Ocean, 84, 125-158 (1967).

32. DASHKIN, N.I. and Yu. G. Chindonova, Mesopelagic Fishes as Resonance Scatterers in the Deep-Scattering Layers of the Atlantic Ocean, Oceanology, 11, No. 10, 404-413 (1971).

33. MACHAN, R. and K. Fedra, A New Towed Underwater Camera System for Wide-Range Benthic Surveys, Marine Biology, 33, 75-84 (1975).

34. MAYNARD, Sherwood D., Fletcher V. Riggs, and John F. Walter, Mesopelagic Micronekton in Hawaiian Waters: Faunal Composition, Standing Stock, and Diel Vertical Migration, Fishery Bulletin, 73, 726-736 (1975).

35. MERRETT, R. and H.S.J. Roe, Patterns & Selectivity in the Feeding of Certain Mesoplegagic Fishes, Marine Biology, 28, 115-126 (1974).

36. MURPHREE, L., C.C. Taylor, and R.W. McClendon, Mathematical Modeling for the Detection of Fish by an Airborne Laser, AIAA Journal, 12, 1606-1692 (1974).

37. NELSON, Joseph S. Fishes of the World, 416 pgs., (1976).

38. PAXTON, John R., A Distributional Analysis for the Lantern Fishes Family Myctophidae of the San Pedro Basin, California, Copeia, No. 2, 422-440 (1967).

39. RICE, Dale W. The Great Blue Whale, Pacific Research, 6, No. 6, 8-10 (1972).

40. ROE, H.S.J., Observations on the Diurnal Vertical Migrations of an Oceanic Animal Community, Marine Biology, 28, 99-113 (1974).

41. RUSSEL, Sir Fredrick S. and Sir Maurice Yonge. The Seas, ix + 283 p, Frederick Warne, Inc., New York (1975).

42.. SEIDEL, W.R. Technical Conference on Fish Finding, Purse Seining and Aimed Trawling, Reykjavik, 24-30 May 1970, Food & Agricultural Organization of the United Nations, FII: FF/70/8, 7

43. SEIDEL, Wilber R. System Specification of Remote Underwater Fisheries Assessement System (RUFAS), U. S. Department of Commerce, National Oceanic and Atmoshperic Administration, National Marine Fisheries Service, Exploratory Fishing & Gear Research Base, Pascagoula, Mississippi 39567.

44. TURNER, H.J. Jr., and B. Prindle, The Vertical Distribution of Fish Bites on Deep Sea Mooring Lines in the Vicinity of Bermuda, ONR Contract Nonr-41500(00), WHOI 67-58 (AD 660 046), Woods Hole Oceanographic Institution, Woods Hole, MA (1967).

45. VENT, R.J. and G.V. Pickwell, Acoustic Volume Scattering Measurements With Related Biological and Chemical Observations in the Northeastern Tropical Pacific, Report No. NUC TP 525, Naval Under-Sea Center, San Diego, California 92132 (1976).

46. WEEKS, Anne, MARMAP - Census of the Sea, NOAA, October, U.S. Department of Commerce, National Oceanic & Atmospheric Administration, Washington, D.C. (1972).

47. Workshop on Problems of Assessing Populations of Nekton, W.G. Pearcy, Ed., Co-sponsored by the Office of Naval Research and the National Science Foundation, 25-27, February 1975, Santa Barbara, California, Final Report No. ACR 211, iv + 30 pgs., Office N. Research, Arlington, Virginia 22217 (1975).

GENERAL

SENSORS, INC.